

# Two Arabidopsis Genes (*IPMS1* and *IPMS2*) Encode Isopropylmalate Synthase, the Branchpoint Step in the Biosynthesis of Leucine<sup>1</sup>[W][OA]

Jan-Willem de Kraker, Katrin Luck, Susanne Textor, James G. Tokuhisa<sup>2</sup>, and Jonathan Gershenzon\*

Max Planck Institute for Chemical Ecology, Beutenberg Campus, D-07745 Jena, Germany

Heterologous expression of the Arabidopsis (*Arabidopsis thaliana*) *IPMS1* (At1g18500) and *IPMS2* (At1g74040) cDNAs in *Escherichia coli* yields isopropylmalate synthases (IPMSs; EC 2.3.3.13). These enzymes catalyze the first dedicated step in leucine (Leu) biosynthesis, an aldol-type condensation of acetyl-coenzyme A (CoA) and 2-oxoisovalerate yielding isopropylmalate. Most biochemical properties of *IPMS1* and *IPMS2* are similar: broad pH optimum around pH 8.5, Mg<sup>2+</sup> as cofactor, feedback inhibition by Leu,  $K_m$  for 2-oxoisovalerate of approximately 300  $\mu\text{M}$ , and a  $V_{\text{max}}$  of approximately  $2 \times 10^3 \mu\text{mol min}^{-1} \text{g}^{-1}$ . However, *IPMS1* and *IPMS2* differ in their  $K_m$  for acetyl-CoA (45  $\mu\text{M}$  and 16  $\mu\text{M}$ , respectively) and apparent quaternary structure (dimer and tetramer, respectively). A knockout insertion mutant for *IPMS1* showed an increase in valine content but no changes in Leu content; two insertion mutants for *IPMS2* did not show any changes in soluble amino acid content. Apparently, in planta each gene can adequately compensate for the absence of the other, consistent with available microarray and reverse transcription-polymerase chain reaction data that show that both genes are expressed in all organs at all developmental stages. Both encoded proteins accept 2-oxo acid substrates in vitro ranging in length from glyoxylate to 2-oxohexanoate, and catalyze at a low rate the condensation of acetyl-CoA and 4-methylthio-2-oxobutyrates, i.e. a reaction involved in glucosinolate chain elongation normally catalyzed by methylthioalkylmalate synthases. The evolutionary relationship between IPMS and methylthioalkylmalate synthase enzymes is discussed in view of their amino acid sequence identity (60%) and overlap in substrate specificity.

Isopropylmalate synthase (IPMS; EC 2.3.3.13) catalyzes the first dedicated step in Leu biosynthesis, an aldol-type condensation between acetyl-CoA and 2-oxoisovalerate yielding 2-isopropylmalate (Fig. 1). The absence of IPMS and other enzymes of branched-chain amino acid biosynthesis (Leu, Ile, and Val) in monogastric animals has been an important stimulus for the development of herbicides that specifically inhibit the synthesis of branched-chain amino acids in plants with minimal toxicity to animals. Nonetheless, in contrast to Val and Ile, the biosynthesis of Leu in plants is largely unexplored. The available evidence indicates that plants use the pathway depicted in Figure 1, which is the same one found in bacteria and yeast (Singh and Shaner, 1995; Singh, 1999; Coruzzi and Last, 2000).

IPMS activities of plants have been described from crude extracts of maize (*Zea mays*) embryos (Oaks, 1965), thylakoid fractions of spinach (*Spinacia oleracea*) chloroplasts (Hagelstein and Schultz, 1993), and soluble chloroplast-enriched preparations of nasturtium (*Tropaeolum majus*), *Diploaxis tenuifolia*, *Eruca sativa*, and Arabidopsis (*Arabidopsis thaliana*), all members of the Brassicaceae (Falk et al., 2004). The next step in Leu biosynthesis is isomerization of the IPMS product 2-isopropylmalate to 3-isopropylmalate (Fig. 1), but an isopropylmalate isomerase has until now not been described from any plant source. More is known about the penultimate step in Leu biosynthesis since Wittenbach et al. (1994) partially purified an isopropylmalate dehydrogenase from pea (*Pisum sativum*) and showed the inhibition of this enzyme by an herbicide. In addition, a cDNA clone encoding an enzyme that dehydrogenates and decarboxylates 3-isopropylmalate to 4-methyl-2-oxovalerate was isolated from both oil seed rape (*Brassica napus*; Ellerstrom et al., 1992) and potato (*Solanum tuberosum*; Jackson et al., 1993). Transamination of the resulting 2-oxo acid yields the final product Leu (Singh, 1999).

A gene unambiguously encoding IPMS activity has not yet been identified from any plant source, despite the considerable attention devoted to four genes of Arabidopsis (Columbia [Col]-0) that show similarity to *IPMS* sequences of other organisms (e.g. Kroymann et al., 2001; Junk and Mourad, 2002; Field et al., 2004; Textor et al., 2004). A principal reason for this attention is the potential role of these genes in glucosinolate

<sup>1</sup> This work was supported by the Max Planck Society and a Marie Curie Individual Fellowship (MCFI-2002-01677) to J.-W.d.K.

<sup>2</sup> Present address: Department of Horticulture, Virginia Tech, Blacksburg, VA 24061.

\* Corresponding author; e-mail gershenzon@ice.mpg.de; fax 49-3641-57-1302.

The author responsible for distribution of materials integral to the findings presented in this article in accordance with the policy described in the Instructions for Authors ([www.plantphysiol.org](http://www.plantphysiol.org)) is: Jonathan Gershenzon (gershenzon@ice.mpg.de).

[W] The online version of this article contains Web-only data.

[OA] Open Access articles can be viewed online without a subscription.

[www.plantphysiol.org/cgi/doi/10.1104/pp.106.085555](http://www.plantphysiol.org/cgi/doi/10.1104/pp.106.085555)

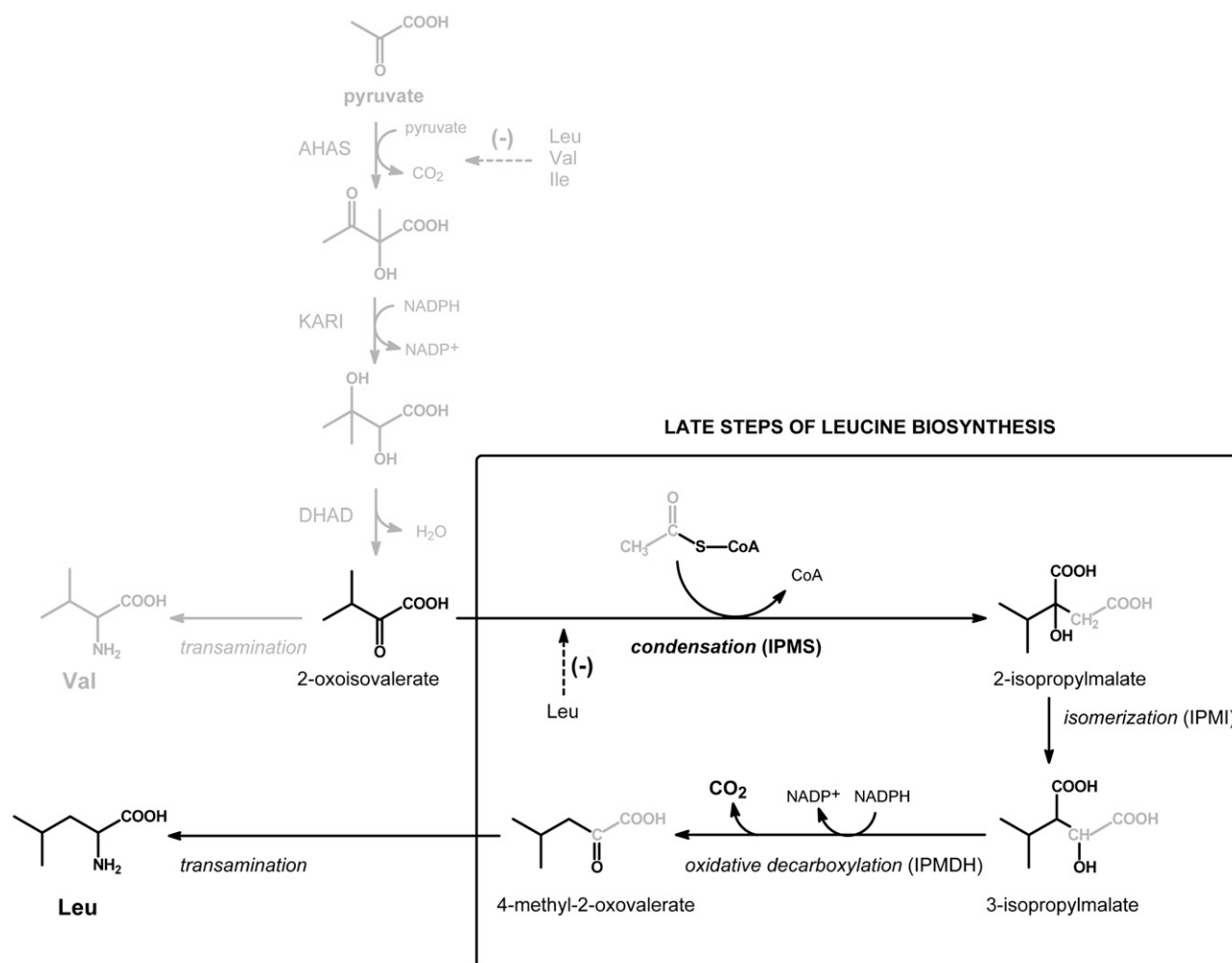


**Figure 1.** The biosynthesis of Leu and Val from pyruvate. The action of aceto-hydroxyacid synthase (AHAS), ketoacid reductoisomerase (KARI), and dihydroxyacid dehydratase (DHAD) yields 2-oxoisovalerate that is either transaminated to Val or subjected to additional reactions specific for Leu biosynthesis. The dedicated step in Leu biosynthesis is the aldol-type condensation between 2-oxoisovalerate and acetyl-CoA that results in formation of 2-isopropylmalate. Isomerization and oxidative decarboxylation by isopropylmalate isomerase (IPMI) and isopropylmalate dehydrogenase (IPMDH) yield 4-methyl-2-oxovalerate that is transaminated to Leu. The enzymes that catalyze the reactions from pyruvate to 2-oxoisovalerate are also involved in biosynthesis of Ile, using 4-oxobutyrate (product of Thr dehydratase) as an initial substrate, but for simplicity have not been depicted. AHAS and IPMS are subject to feedback inhibition as shown with dashed lines.

biosynthesis. Two of these *IPMS*-like sequences (At5g23010 and Atg5g23020) are located at the *GS-Elong* locus on chromosome V, which regulates the side-chain length of the aliphatic glucosinolates in Arabidopsis (Campos de Quiros et al., 2000; Kroymann et al., 2001, 2003).

Glucosinolates are amino acid-derived plant secondary metabolites (formed mainly from Met, Trp, and Phe in Arabidopsis) that consist of a  $\beta$ -thio-Glc moiety, a sulfonated oxime, and a variable side chain formed from the parent amino acid. In the case of the Met-derived glucosinolates, the side chain of the amino acid is elongated by up to six methylene groups prior to biosynthesis of the glucosinolate backbone (Fig. 2), resulting in the formation of products with C<sub>3</sub> to C<sub>8</sub> side chains (Wittstock and Halkier, 2002; Halkier and

Gershenzon, 2006). In the iterative, three-step elongation process demonstrated in *in vivo* feeding studies, transaminated Met (4-methylthio-2-oxobutyrate) is subject to the same type of reactions (Fig. 2) that convert 2-oxoisovalerate into Leu (Fig. 1; Chisholm and Wetter, 1964; Matsuo and Yamazaki, 1968; Serif and Schmotzer, 1968; Graser et al., 2000). Each cycle of elongation is initiated by an aldol-type condensation between acetyl-CoA and a  $\omega$ -methylthio-2-oxo acid leading to the formation of a  $\omega$ -methylthioalkylmalate. Both *IPMS*-like sequences at the *Gs-Elong* locus of Arabidopsis Col-0 were shown to encode proteins that possess this activity, but each had only very limited *IPMS* activity (Kroymann et al., 2001; Textor et al., 2004; S. Textor, unpublished data). Therefore, the genes were called methylthioalkylmalate synthase (*MAM*)

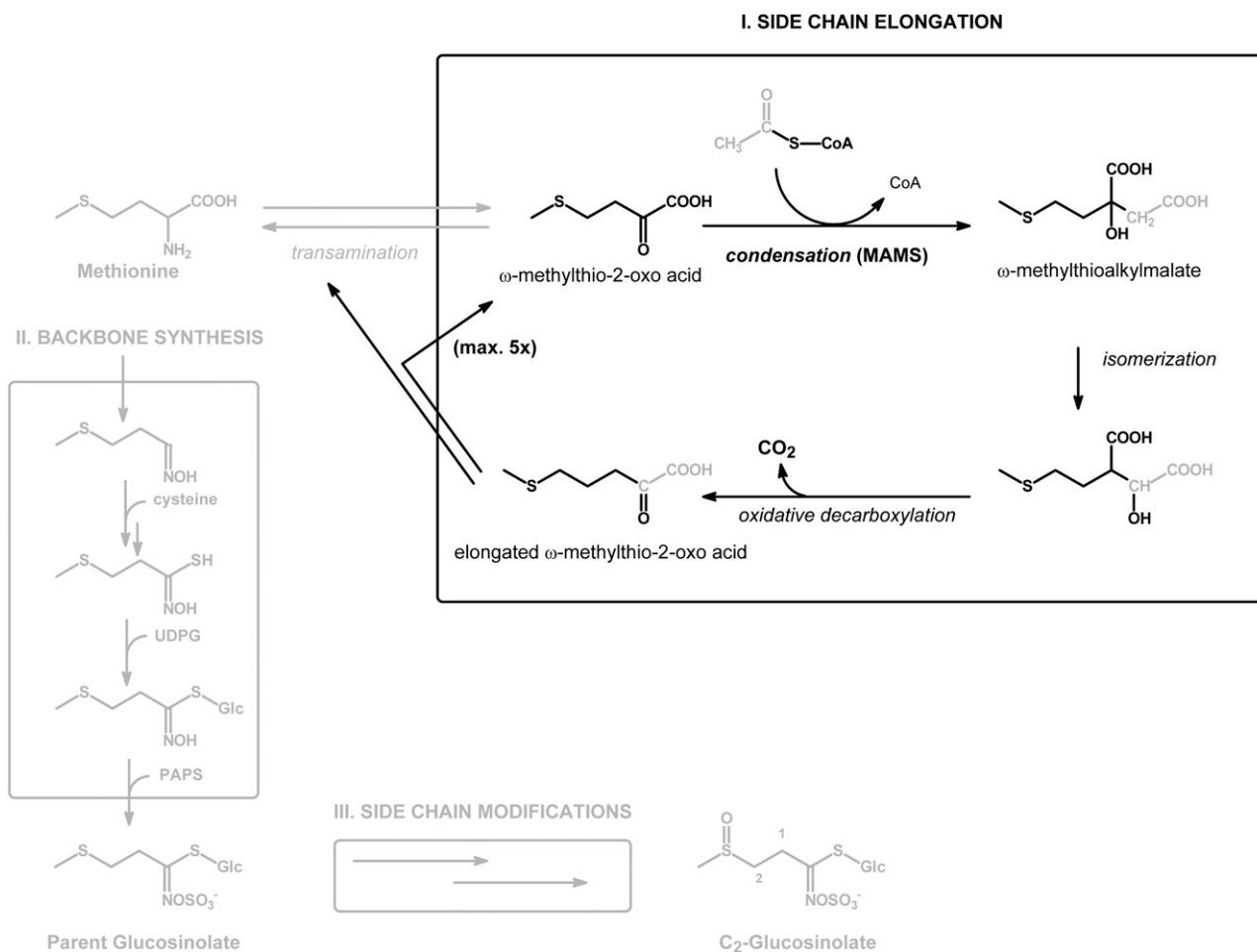


**Figure 2.** General scheme for the biosynthesis of aliphatic glucosinolates involving Met side-chain elongation (I), backbone synthesis (II), and side-chain modifications (III). The proposed cycle for side-chain elongation of deaminated Met (I) commences with an aldol-type condensation between the respective  $\omega$ -methylthio-2-oxo acid and acetyl-CoA, a reaction catalyzed by MAM. The methylthioalkylmalate product is converted through subsequent isomerization and oxidative decarboxylation into a  $\omega$ -methylthio-2-oxo acid that is elongated by one methylene group. The elongated  $\omega$ -methylthio-2-oxo acid is either transaminated and enters glucosinolate backbone synthesis (II) or undergoes additional cycles of side-chain elongation. Glucosinolate backbone synthesis is represented in a simplified manner without the identified enzymes and cofactors. The depicted end product, 2-methylsulfinyethyl glucosinolate, is a C<sub>2</sub>-glucosinolate that has not been side-chain elongated and does not occur naturally in Arabidopsis.

genes, specifically, *MAM1* and *MAM3* (also known as *MAM-L*). A third *MAM* gene, *MAM2*, has been described from other Arabidopsis ecotypes (Kroymann et al., 2003). Analysis by Field et al. (2004) of a *MAM3* knockout line from Arabidopsis showed the absence of long-chain glucosinolates (C<sub>6</sub>, C<sub>7</sub>, and C<sub>8</sub>), confirming the role of *MAM3* in glucosinolate biosynthesis.

The function of the two other *IPMS*-like sequences, located at opposite ends of chromosome I (At1g18500 and At1g74040), has not yet been clearly determined, though cluster analysis of the deduced amino acid sequences revealed that they are more closely related to one another and to the two reported *IPMS* sequences from wild tomato (*Lycopersicon pennellii*; GenBank accession nos. AAB61598 and AAB61599) than to the *MAM1* or *MAM3* sequences, suggesting they probably encode true *IPMS*s (Kroymann et al., 2001). Just

recently, a *MAM* sequence (GenBank accession no. DQ143886) was reported from *Brassica atlantica* that shares a high amino acid identity (90% and 86%) with the predicted *IPMS* homologs of Arabidopsis and is able to restore the growth of an *IPMS*-null *Escherichia coli* mutant in the absence of Leu (Field et al., 2006), and thus was called an *IPMS* (*BatIMS*). Such a rescue of an *IPMS*-null *E. coli* mutant was also described for At1g74040 and furthermore for both *MAM*-encoding genes, *MAM1* and *MAM3* (Junk and Mourad, 2002; S. Textor, unpublished data). An overview of these confusing, and in part contradictory, results (Table I) makes the point that it is problematic to definitely assign the in planta function of these genes based solely on complementation of an *IPMS*-null *E. coli* mutant strain. Analyses of a knockout mutant in At1g18500 also gave little information about the function of this *IPMS* gene

**Table 1.** Complementation of *IPMS*-null *E. coli* mutant by *IPMS*-like genes of *Arabidopsis*

Complementation indicated by "+," yes; "-", no; or not determined (ND).

AGI Code No.	Name	Junk and Mourad (2002) <sup>a</sup>	Field et al. (2004) <sup>b</sup>	S. Textor (Unpublished Data) <sup>c</sup>	This Article <sup>d</sup>
At1g18500	<i>IPMS1</i>	ND	–	ND	–
At1g74040	<i>IPMS2</i>	–	+	ND	+
At5g23010	<i>MAM1</i>	+	–	ND	ND
At5g23020	<i>MAM3</i>	+	–	+	ND

<sup>a</sup>Conditions not described. <sup>b</sup>Overnight at 37°C. <sup>c</sup>Three days at 28°C. <sup>d</sup>Three days at either 30°C or 37°C.

since neither a significant change in Leu nor in glucosinolate content was detected, and only (pleiotropic?) alterations in Asn, Gln, His, and Val content were observed (Field et al., 2004).

At least one of the two predicted *IPMS* genes at chromosome I of *Arabidopsis*, named *IPMS1* (At1g18500) and *IPMS2* (At1g74040) in this article, should encode an active *IPMS* because such an enzyme activity is absolutely essential to the plant for its synthesis of Leu. In this study, *IPMS1* and *IPMS2* were cloned and heterologously expressed in *E. coli*. Determination of the substrate specificity of the purified proteins in conjunction with analysis of knockout mutant lines reveals that *IPMS1* and *IPMS2* both encode bona fide *IPMS*s involved in Leu biosynthesis and do not participate in the chain elongation of glucosinolates.

## RESULTS

### *IPMS1* and *IPMS2* Have *IPMS* Activity

The open reading frames (ORFs) of *IPMS1* (At1g18500) and *IPMS2* (At1g74040) from *Arabidopsis* were separately cloned without the predicted N-terminal targeting sequence (ChloroP; Emanuelsson et al., 1999) into an expression vector containing a polyhistidine coding domain (His-tag) and expressed in *E. coli*. The recombinant protein was purified over an Ni-NTA agarose affinity column and showed on SDS-PAGE a protein band at the expected size of around 65 kD that was 90% to 95% pure (data not shown); about 4.5 mg of protein was obtained from a 100-mL bacterial culture.

Incubation of 0.5 mM [<sup>14</sup>C]acetyl-CoA and 3 mM 2-oxoisovalerate with 50 μg of partially purified *IPMS* protein for 1 h gave a complete incorporation of the <sup>14</sup>C label into a product that yielded a single peak in the radiodetector trace of the HPLC (Fig. 3A). This product peak coeluted with a synthetic standard of 2-isopropylmalate (Fig. 3C). In these measurements, no difference was detected in enzyme activity between *IPMS1* and *IPMS2*. In the absence of 2-oxo acid substrate, [<sup>14</sup>C]acetyl-CoA was partially hydrolyzed to [<sup>14</sup>C]acetate and CoA (Fig. 3B), probably due to the pH of the enzyme assay and a minor acetyl-CoA hydrolyzing activity of the enzyme itself (see also Table III). Boiled enzyme incubated with 2-oxoisovalerate and [<sup>14</sup>C]acetyl-CoA yielded a similar chromatogram (data

not shown). To check for *MAM* activity associated with formation of chain-elongated, Met-derived glucosinolates, the purified *IPMS* proteins were incubated with 4-methylthio-2-oxobutyrates and [<sup>14</sup>C]acetyl-CoA under the same conditions. However, a much smaller amount of [<sup>14</sup>C]-2-(2'-methylthio)ethylmalate was measured compared to the amount of 2-isopropylmalate formed from 2-oxoisovalerate, and most of the [<sup>14</sup>C]acetyl-CoA remained (Fig. 3D). These data suggest that the *IPMS1* and *IPMS2* genes are much more likely to serve as *IPMS*s in Leu biosynthesis than in the formation of methylthioalkylmalate compounds for glucosinolate biosynthesis.

Additional support for the function of the *IPMS2*-encoded protein comes from the observation that it is able to complement the *IPMS*-null *E. coli* strain CV512(DE3). This bacterium was not able to grow on a minimal medium without supplemented amino acids, unless it had been transformed with a construct carrying either the *E. coli IPMS* gene *leuA* or the *IPMS2* gene from *Arabidopsis*. Transcription of the gene construct was induced with isopropyl-β-galactoside (IPTG), and both the *E. coli leuA* transformant (positive control) and the *IPMS2* transformant grew at 30°C within 3 d, whereas no bacterial growth was observed for CV512(DE3) alone (data not shown). Growth of the *IPMS2* transformant was less at 37°C. In contrast to this experiment, our attempts to complement CV512(DE3) with the *IPMS1* construct were unsuccessful.

### *IPMS1* and *IPMS2* Have Similar But Not Identical Biochemical Characteristics

*IPMS1* and *IPMS2* activity not only depended upon the presence of a 2-oxo acid substrate and acetyl-CoA, but also required Mg<sup>2+</sup> in millimolar concentrations (Fig. 4A). Hence, 4 mM Mg<sup>2+</sup> was added routinely to the incubations. Quantitative measurements using an endpoint assay with 5,5'-dithiobis(2-nitrobenzoic acid) (DTNB; see "Materials and Methods") showed a 75% to 95% loss of enzyme activity when the His-tag purified protein was desalted into a buffer without Mg<sup>2+</sup> and then incubated in the absence of Mg<sup>2+</sup>. Enzyme activity was completely lost in the presence of 10 mM EDTA. The residual enzyme activity in the absence of Mg<sup>2+</sup> (monitored with the radio-HPLC assay)

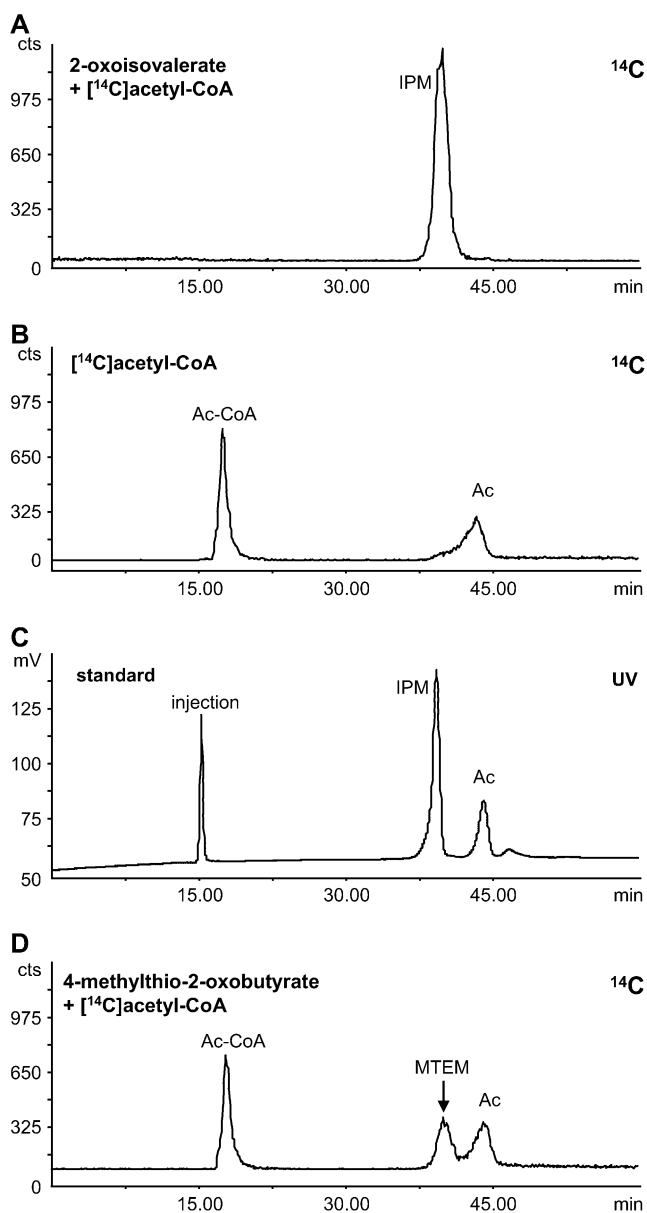


**Figure 3.** Radio-HPLC analyses of the biochemical assay for IPMS2. Results for IPMS1 had a similar pattern. A, Incubation of IPMS2 with 500  $\mu\text{M}$  [ $^{14}\text{C}$ ]acetyl-CoA and 3 mM 2-oxoisovalerate shows [ $^{14}\text{C}$ ]2-isopropylmalate (IPM) as the only radioactive labeled product. B, In the absence of 2-oxo acid substrate, a small amount of [ $^{14}\text{C}$ ]acetate (Ac) is formed, whereas most of the [ $^{14}\text{C}$ ]acetyl-CoA (Ac-CoA) remains intact and is hardly retained in the HPLC column. C, UV trace (230 nm) of the HPLC showing the elution pattern of a standard solution containing 10 mM acetic acid (Ac) and 5 mM 2-isopropylmalate (IPM), and the injection peak at 15 min. D, Incubation of the IPMS2 gene product with 4-methylthio-2-oxobutyrate and [ $^{14}\text{C}$ ]acetyl-CoA yields a small amount of [ $^{14}\text{C}$ ]2-(2'-methylthio)ethylmalate (MTEM), whereas most of the [ $^{14}\text{C}$ ]acetyl-CoA (Ac-CoA) remains.

was also completely lost if the incubation assay was adjusted to 4 mM  $\text{Ca}^{2+}$ ,  $\text{Cu}^{2+}$ ,  $\text{Ni}^{2+}$ , or  $\text{Zn}^{2+}$ , whereas the residual activity was not inhibited by the presence of 4 mM  $\text{Fe}^{2+}$  or  $\text{Co}^{2+}$ . While 4 mM  $\text{K}^{+}$  gave a slight stimulation of the residual enzyme activity and the ad-

dition of 4 mM  $\text{Mn}^{2+}$  restored about 50% of the initial activity, only the addition of 4 mM of  $\text{Mg}^{2+}$  brought the enzyme activity back to its full initial rate.

The pH curves of IPMS1 and IMPS2 are similar and display rather broad optima around pH 8.5 (Fig. 4B). The more flattened curve for IPMS2 with a sharp drop of enzyme activity above pH 9.5 was seen consistently in replicate experiments. A pH of 8.0 was routinely used in enzyme assays to minimize the spontaneous chemical hydrolysis of acetyl-CoA that increased noticeably above this value.

The molecular mass of the native recombinant protein was determined by gel filtration on a calibrated Superdex-200 column, assaying the activity of eluted 1-mL fractions by the DTNB method (Fig. 4C). The main activity of IPMS1 eluted at a molecular mass of 124 kD, suggesting that the functional protein is a dimer, as the monomer size calculated from the amino acid sequence is 63.1 kD (including the additional 0.8 kD from the His-tag). On the other hand, the main activity of IPMS2 eluted at approximately 280 kD, indicating this enzyme is active as a tetramer (predicted monomer size 64.1 kD). Omitting the 150 mM of NaCl from the elution buffer or adding 2 mM  $\text{MgCl}_2$  to the elution buffer did not affect these results.

Enzyme kinetics were determined in a continuous spectrophotometric assay with *N*-ethylmaleimide (NEM; see "Materials and Methods") and are presented in Table II. The main difference between IPMS1 and IPMS2 was the  $K_m$  obtained for acetyl-CoA: 45  $\mu\text{M}$  and 16  $\mu\text{M}$ , respectively. There was no significant difference observed in the  $K_m$  for 2-oxoisovalerate (304  $\mu\text{M}$  and 279  $\mu\text{M}$ ), nor any difference in specific activity between IPMS1 and IPMS2.

IPMS activity in plants is generally considered to be feedback inhibited by Leu (Singh, 1999; Coruzzi and Last, 2000). To test this possibility, aliquots of the incubation mixture were adjusted to Leu concentrations between 0.025 mM and 10 mM. We detected a slight inhibitory effect of Leu on the activity of IPMS1 and IPMS2 (Fig. 5). Inhibition of both enzymes reached a maximum of 30% to 35% around 1 mM Leu, but declined to 15% at higher concentrations of Leu in the case of IPMS2. Changing the pH of the incubation mixture to 7.5 did not augment the inhibitory effect of Leu as had been observed for the IPMS of yeast (Ulm et al., 1972). To account for the possible influences of posttranscriptional modifications of the IPMS proteins in planta, the effect of Leu was also tested on the IPMS activity present in crude extracts of Arabidopsis. An extract prepared from leaf material (3.5 weeks old) according to the protocol of Textor et al. (2004), but leaving out the ammonium-sulfate precipitation step, was measured in the presence of an acetyl-CoA regenerating system. The inhibitory effect of Leu on the IPMS activity present in the crude extract was similar to those values measured for the heterologously expressed IPMSs: 14% at 0.5 mM Leu, 33% at 1.0 mM Leu, and 48% at 5.0 mM Leu. No inhibitory effects on the

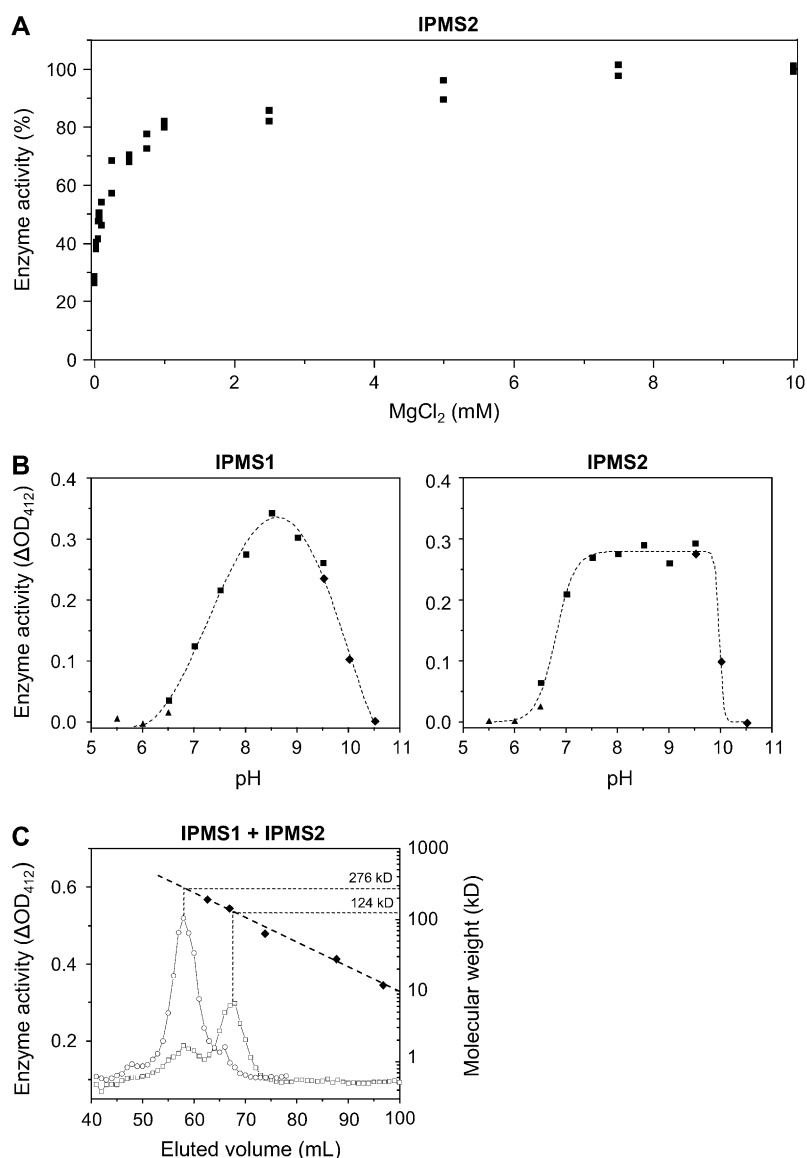


**Figure 4.** Properties of Arabidopsis IPMSs. A, Effect of MgCl<sub>2</sub> concentration on IPMS2 activity; 0 mM corresponds to a desalted enzyme preparation without addition of MgCl<sub>2</sub>. A similar graph was obtained for IPMS1. B, pH Curves for enzyme activity of IPMS1 and IPMS2 using MES (▲), BisTris-propane (■), and 2-amino-2-methyl-1-propanol (◆). Each data point corresponds to a duplicate enzyme activity measurement with DTNB that is corrected for chemical hydrolysis of acetyl-CoA at each particular pH value. C, Determination of the molecular mass of IPMS1 (□) and IPMS2 (○) by calibrated gel-filtration chromatography. The column was calibrated by measuring the elution volume (◆) of β-amylase (200 kD), alcohol dehydrogenase (150 kD), bovine serum albumin (66 kD), carbonic anhydrase (29 kD), and cytochrome C (12.4 kD). The void volume of the column determined with Blue Dextran (2.0 × 10<sup>3</sup> kD) was 44 mL.

crude IPMS enzyme were observed for Ile, Val, and Gly. In previous work, the IPMS of spinach was reported to be 100% inhibited by micromolar concentrations of Leu (Hagelstein and Schultz, 1993). However, our experiments on the IPMS activity present in a chloroplast-enriched crude extract of spinach prepared after Falk et al. (2004), without the gel-filtration step, did not show such a pronounced effect. The inhibition of IPMS activity was similar to that seen with

the Arabidopsis crude extract: 32% at 0.5 mM Leu, 42% at 1 mM Leu, and 66% at 5 mM Leu.

#### Both Enzymes Accept Other Substrates and Catalyze the First Condensation Reaction of Glucosinolate Chain Elongation at Low Rates

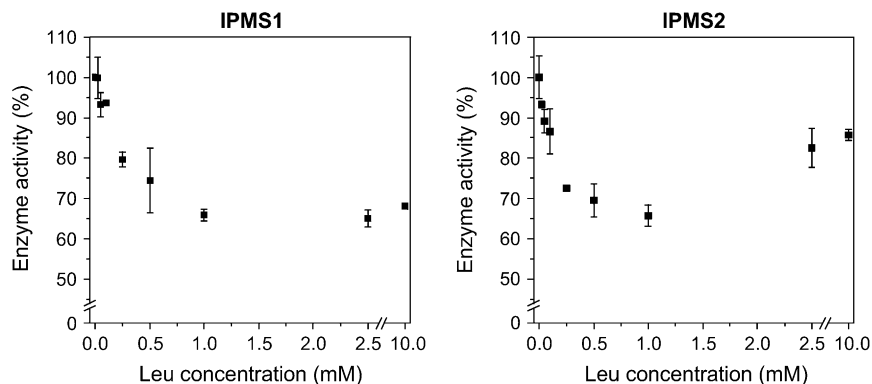
The detectable conversion of 4-methylthio-2-oxobutyrate to its alkylmalate derivative by IPMS1

**Table II.** Kinetic parameters for IPMS1 and IPMS2

Enzyme	Substrate	$K_m$ ( $\mu\text{M}$ ) $\pm$ SE	$V_{\text{max}}$ ( $\mu\text{mol min}^{-1} \text{g}^{-1}$ ) $\pm$ SE	$k_{\text{cat}}$ ( $\text{s}^{-1}$ )	$k_{\text{cat}}/K_m$ ( $\text{M}^{-1} \text{s}^{-1}$ )
IPMS1	2-Oxoisovalerate <sup>a</sup>	304 $\pm$ 68	2.3 $\times$ 10 <sup>3</sup> $\pm$ 0.2 $\times$ 10 <sup>3</sup>	2.4	7.8 $\times$ 10 <sup>3</sup>
	Acetyl-CoA <sup>b</sup>	45 $\pm$ 10	2.1 $\times$ 10 <sup>3</sup> $\pm$ 0.1 $\times$ 10 <sup>3</sup>	2.2	4.7 $\times$ 10 <sup>4</sup>
IPMS2	2-Oxoisovalerate <sup>a</sup>	279 $\pm$ 51	2.2 $\times$ 10 <sup>3</sup> $\pm$ 0.1 $\times$ 10 <sup>3</sup>	2.3	8.3 $\times$ 10 <sup>3</sup>
	Acetyl-CoA <sup>b</sup>	16 $\pm$ 4	1.8 $\times$ 10 <sup>3</sup> $\pm$ 0.1 $\times$ 10 <sup>3</sup>	1.9	1.2 $\times$ 10 <sup>5</sup>

<sup>a</sup>Measured in the presence of 500  $\mu\text{M}$  acetyl-CoA. <sup>b</sup>Measured in the presence of 1 mM 2-oxoisovalerate.

**Figure 5.** Leu inhibition of the heterologously expressed IPMS1 and IPMS2 from Arabidopsis.



and IPMS2 from Arabidopsis (Fig. 3) led us to test various 2-oxo acid substrates other than 2-oxoisovalerate. Potential substrates were incubated with [ $^{14}$ C]acetyl-CoA at saturating concentrations and the reaction mixtures analyzed by radio-HPLC. The reaction products were identified by coelution of synthetic standards and/or liquid chromatography-mass spectrometry analyses (Kroymann et al., 2001; Textor et al., 2004; S. Textor, unpublished data). The enzymatic rates for converted substrates were determined with DTNB in a timed enzyme assay and are expressed relative to the conversion of 2-oxoisovalerate (Table III). The specific activities for IPMS determined in this way are comparable to those in Table II that were determined with NEM in the less-sensitive continuous spectrophotometric assay.

There was no major difference between IPMS1 and IPMS2 with respect to their substrate specificities. Of the tested substrates, 2-oxobutyrate seems to perform as well or even better than the true substrate 2-oxoisovalerate (common name for 3-methyl-2-oxobutyrate), while pyruvate and 2-oxovalerate were also converted in ample yield. However, 3-methyl-2-oxovalerate and 4-methyl-2-oxovalerate, i.e. transaminated products of Ile and Leu, respectively, were converted only in trace amounts, while phenylpyruvate, the 2-oxo acid of Phe, was not converted at all. The reaction between 4-methylthio-2-oxobutyrate and acetyl-CoA occurred at a relatively low yield (consistent with the data in Fig. 3), but was 3 to 4 times more efficient than the enzymatic conversion of its methylene analog, 2-oxohexanoate. As mentioned in the introduction, formation of 2-(2'-methylthio)ethylmalate represents the aldol-type condensation reaction in the first cycle of Met side-chain elongation and yields a direct precursor of  $C_3$ -glucosinolate biosynthesis. However, this reaction proceeds at a far slower rate than the conversion of 2-oxoisovalerate to isopropylmalate. Estimations by the DTNB assay gave a  $K_m$  value of at least 3 mM for 4-methylthio-2-oxobutyrate that results in a specificity constant ( $k_{cat}/K_m$ ) of less than  $13 \text{ M}^{-1} \text{ s}^{-1}$ . The  $K_m$  for pyruvate was in the millimolar range as well. Substrates having a carbon chain longer than 4-methylthio-2-oxobutyrate or 2-oxohexanoate were not accepted at all.

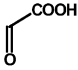
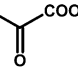
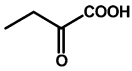
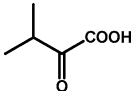
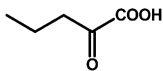
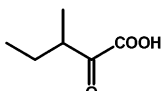
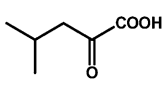
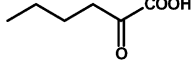
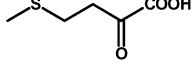
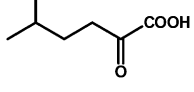
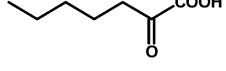
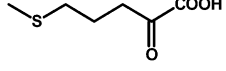
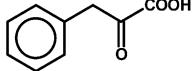
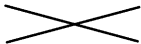
To shed further light on whether IPMS1 and IPMS2 participate in glucosinolate formation, we investigated whether or not the low activity of these enzymes with 4-methylthio-2-oxobutyrate is a general feature of the IPMS enzymes. When the substrate specificity of the IPMS cloned from *E. coli* (the *leuA* gene) was measured by incubation of the purified His-tag protein with [ $^{14}$ C]acetyl-CoA, the substrates 4-methylthio-2-oxobutyrate, pyruvate, and 2-oxovalerate were converted to their malate derivatives to the same extent relative to 2-oxoisovalerate as observed for the IPMSs of Arabidopsis (Supplemental Fig. S1).

#### Plant Lines Mutated in *IPMS1* and *IPMS2* Still Had Wild-Type Levels of Leu

To determine how the *IPMS* genes contribute to amino acid and glucosinolate biosynthesis, we characterized three mutant lines of Arabidopsis (Col-0), one with a T-DNA insertion in the *IPMS1* gene (Salk\_101771) and two with a T-DNA insertion in the *IPMS2* gene (Salk\_051060 and Salk\_000074; Alonso et al., 2003). The genomic DNA of individuals from crosses segregating for each insert were tested for the presence of a T-DNA insert in the respective genes using oligonucleotide primer pairs derived from the T-DNA insert and the respective *IPMS* genes (Supplemental Table S1), and the product sizes and sequences obtained were consistent with the reported insertion sites (Supplemental Fig. S2). Individual plants were identified that were homozygous for the T-DNA insert, heterozygous, or lacking the T-DNA insert (outsegregants).

As shown in Figure 6, transcripts for *IPMS1* and *IPMS2* were readily detected in wild-type plants by reverse transcription (RT)-PCR, but no transcript of *IPMS1* was detected in homozygotes for insertion in this gene (Salk\_101771 line). In homozygotes for the *IPMS2* insertions, no *IPMS2* transcript was observed in the Salk\_051060 line, and only a weak band for *IPMS2* was detected in homozygotes for the Salk\_000074 line. In the mutant lines for each *IPMS* gene, transcript of the other *IPMS* gene was present, but no compensatory effects were observed. The *IPMS1* mutant line grew somewhat slower and had undulated leaves that tended to be slightly chlorotic as

**Table III.** Substrate specificity of IPMS1 and IPMS2

Substrate <sup>a</sup>	Structure	Elongation Step <sup>b</sup>	Relative Conversion <sup>c</sup> (%) ± SD	
			IPMS1	IPMS2
Glyoxylate			0.3 ± 0.0	0.2 ± 0.1
Pyruvate			12.7 ± 1.8	15.7 ± 1.2
2-Oxobutyrate			112.2 ± 2.3	97.5 ± 2.7
<b>2-Oxoisovalerate</b>			<b>100.0 ± 5.6</b>	<b>100.0 ± 3.5</b>
2-Oxovalerate			27.2 ± 0.8	33.8 ± 2.0
3-Methyl-2-oxovalerate			0.6 ± 0.0	0.5 ± 0.1
4-Methyl-2-oxovalerate			0.7 ± 0.1	1.1 ± 0.1
2-Oxohexanoate			0.5 ± 0.0	0.5 ± 0.0
4-Methylthio-2-oxobutyrate		C <sub>2</sub> → C <sub>3</sub>	1.3 ± 0.1	1.7 ± 0.1
5-Methyl-2-oxohexanoate			–	–
2-Oxoheptanoate			–	–
5-Methylthio-2-oxopentanoate		C <sub>3</sub> → C <sub>4</sub>	–	–
Phenylpyruvate			–	–
Absence of 2-oxo-substrate <sup>d</sup>			0.4 ± 0.0	0.6 ± 0.0

<sup>a</sup>Incubations were done with 20 mM 2-oxo acid and 500 μM acetyl-CoA. <sup>b</sup>Reaction of these substrates leads to glucosinolates with the indicated change in number of carbon atoms in the side chain. <sup>c</sup>100% Enzyme activity corresponds to a specific activity of  $2.6 \times 10^3 \mu\text{mol}^{-1} \text{min}^{-1} \text{g}^{-1}$  for IPMS1 and  $2.9 \times 10^3 \mu\text{mol}^{-1} \text{min}^{-1} \text{g}^{-1}$  for IPMS2. <sup>d</sup>Represents the hydrolysis of acetyl-CoA due to the presence of enzyme without 2-oxo acid substrate; this value was taken as a blank for all measurements.



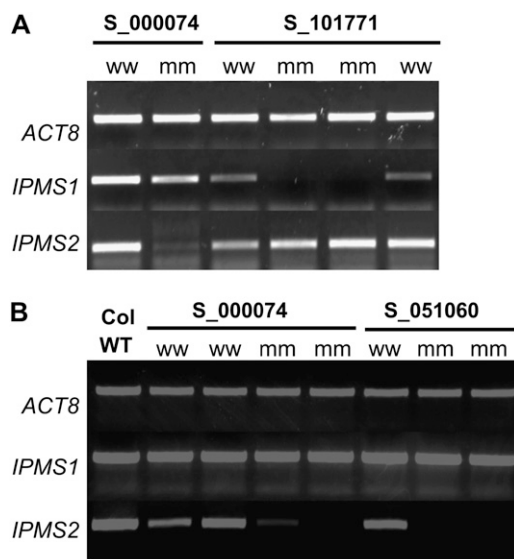


**Figure 6.** Semi-quantitative RT-PCR analyses of *IPMS* transcript levels in leaf tissues of Salk T-DNA insertion lines, homozygous (mm) for the insertion or lacking the insertions (ww), and Col-0 wild type (WT). A, Results for the *IPMS1* mutant line S\_101771 compared to the *IPMS2* mutant line S\_000074; B, results for the *IPMS2* mutant lines S\_000074 and S\_051060.

compared to its outsegregant. However, the *IPMS2* mutants had a normal appearance.

Amino acid analyses of 3- to 4-week-old rosettes of the *IPMS1* mutant (Salk\_101771 [mm]; Fig. 7A) showed an increase in the content of the aliphatic amino acid Val from  $1,662 \pm 236$  pmol mg<sup>-1</sup> dry weight to  $2,919 \pm 639$  pmol mg<sup>-1</sup> dry weight. No significant change in any other measured amino acid was observed compared to the controls (Col-0 wild type and the Salk\_101771 outsegregant). The *IPMS2* mutants (Salk\_000074 and Salk\_051060; Fig. 7B) showed no significant differences in amino acid content compared with their respective controls. The rosettes of the three mutant lines and their controls were also analyzed for their glucosinolate content, but no significant changes were observed either in quantity or quality (Supplemental Fig. S3).

#### Both Genes Are Expressed Constitutively throughout the Plant

Semi-quantitative RT-PCR analysis revealed that both *IPMS* genes are expressed throughout the plant and mRNA transcript levels do not differ extensively between various organs (Supplemental Fig. S4). These results are consistent with data from the Arabidopsis ATH1 Genome Array (Affymetrix), posted on the Internet and retrieved with the GENEVESTIGATOR program (Zimmermann et al., 2004). The collected microarray data also show that both *IPMS* genes are similarly expressed among different developmental stages and after specific stress treatments (Supplemental Fig. S5). An exception is the level of *IPMS1* tran-

script in the seeds during silique ripening, which is at least twice as high as in most other plant tissues.

#### DISCUSSION

##### *IPMS1* and *IPMS2* Function in Leu Formation But Not in Glucosinolate Biosynthesis

Heterologous expression of the Arabidopsis *IPMS1* (At1g18500) and *IPMS2* (At1g74040) cDNAs in *E. coli* and the study of the enzymatic properties of the protein products demonstrated that both genes encode IPMSs, which catalyze the aldol-type condensation reaction between acetyl-CoA and 2-oxoisovalerate in the biosynthesis of Leu. Nonetheless, both proteins were also able to catalyze the MAM reaction between acetyl-CoA and 4-methylthio-2-oxobutyrate to some extent. However this reaction occurs with such a low specificity constant ( $k_{\text{cat}}/K_m < 13 \text{ M}^{-1} \text{ s}^{-1}$ ) in comparison with the previously measured value for MAM3 ( $1.4 \times 10^3 \text{ M}^{-1} \text{ s}^{-1}$ ; S. Textor, unpublished data) that this MAM activity is probably of no significance in vivo. In addition, an insertion mutant for *IPMS1* with undetectable transcript levels of *IPMS1* (Salk\_101771), an insertion mutant for *IPMS2* with undetectable transcript levels of *IPMS2* (Salk\_051060), and an *IPMS2* insertion mutant line with reduced *IPMS2* transcript levels (Salk\_000074) all did not display any changes in glucosinolate content (Supplemental Fig. S3). Hence, we conclude that *IPMS1* and *IPMS2* have a primary function in Leu biosynthesis and are not significantly involved in the Met side-chain elongation of glucosinolate biosynthesis.

In accordance with this conclusion, the *IPMS2* gene in a prokaryotic expression construct rescued the *IPMS*-null *E. coli* mutant strain CV512(DE3), but curiously an *IPMS1* construct did not. Rescue of the Leu-deficient *E. coli* strain by *IPMS2*, but not *IPMS1*, was also observed by Field et al. (2004); however, Junk and Mourad (2002) could not demonstrate any complementation with *IPMS2*, but did for *MAM1* and *MAM3* (see also Table I). The inconsistencies in demonstrating the ability of these plant genes to complement the Leu auxotrophy in *E. coli* provide a cautionary tale about the value of complementation assays as surrogates for a full characterization of in vitro enzyme activity.

Amino acid analysis of the *IPMS1* and *IPMS2* insertion mutants also gave equivocal results about in vivo function, since none of the insertion mutants showed any changes in soluble Leu content (Fig. 7). As plants require Leu for survival, a total lack of Leu accumulation was not expected in these viable mutant lines. Nevertheless, the absence of any detectable change in Leu content is noteworthy and must demonstrate that *IPMS1* and *IPMS2* compensate for each other's absence very well, because it is unlikely that the MAM enzymes with their very low IPMS activity can contribute to Leu biosynthesis in an efficient way (S. Textor, unpublished data).

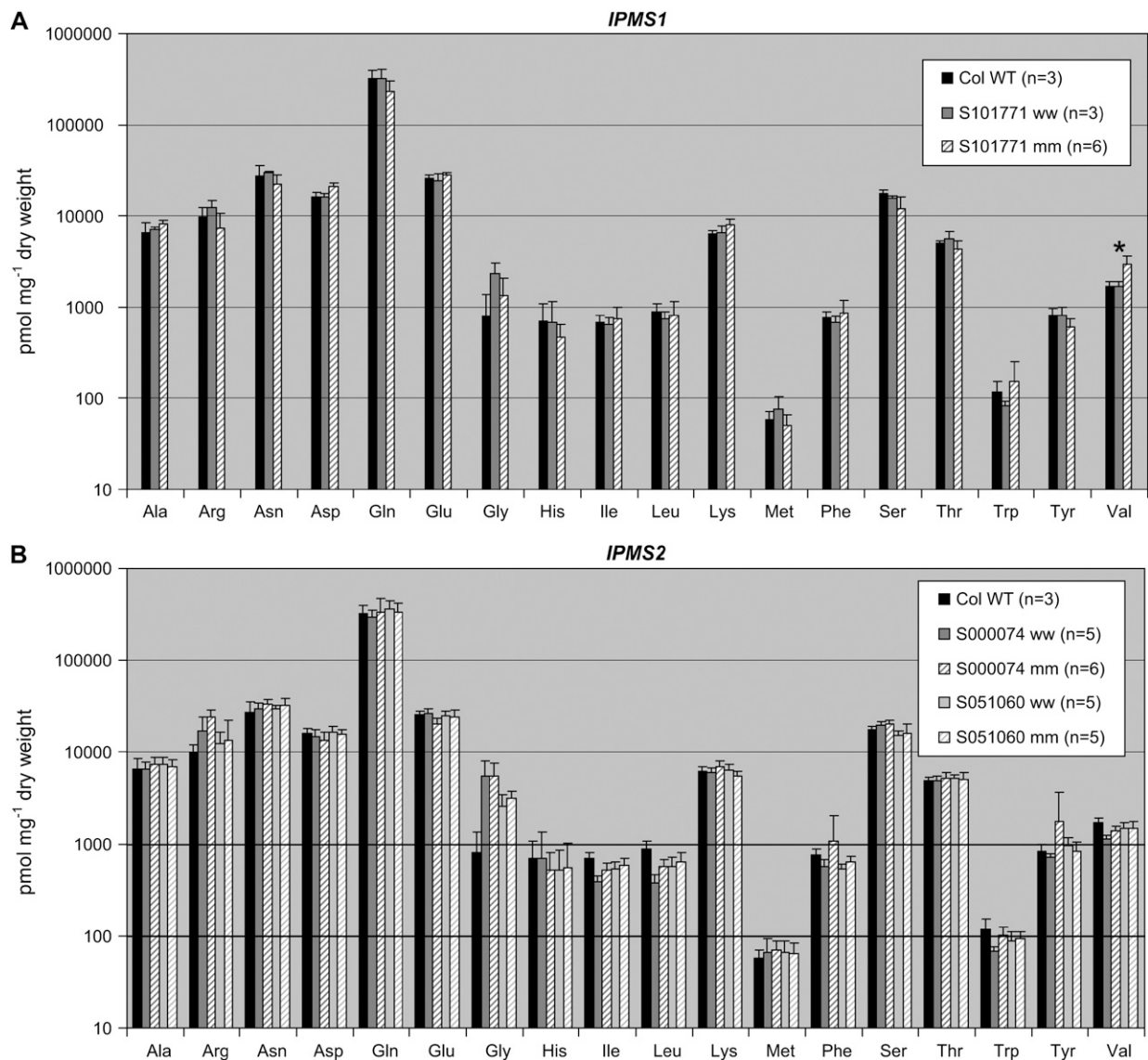


**Figure 7.** Analyses of the free amino acid content of homozygous T-DNA insertion lines for *IPMS1* (A; Salk\_101771 [mm]) and *IPMS2* (B; Salk\_051060 [mm] and Salk\_000074 [mm]). The *IPMS1* mutant shows a significant increase in Val content in comparison with the corresponding outsegregants (ww) and Col-0 wild type. Error bars indicate sd.

Despite the lack of a reduction in Leu, the *IPMS1* insertion mutant has a clear phenotype in its elevated soluble Val content (Fig. 7). Such an increase in Val content was also observed in an independently generated *En-1* insertion mutant of *IPMS1* by Field et al. (2004), but was not discussed any further. This feature may be a consequence of the fact that the *IPMS1* mutant—despite the presence of *IPMS2*—has less IPMS activity relative to Val-aminotransferase activity than found in wild-type plants. Since both enzymes use 2-oxoisovalerate as a substrate, such an imbalance will increase the amount of Val at the expense of Leu. This will reduce the feedback inhibition of acetoacetyl-CoA synthase (AHAS), because Val is a less potent inhibitor of AHAS activity than Leu and, moreover, it is actually the combination of Leu and Val that has the strongest

inhibitory effect on AHAS (Mifflin and Cave, 1972; Lee and Duggleby, 2001). Such a scenario may account for the maintenance of normal levels of Leu in the *IPMS1* insertion mutant, despite lower quantities of IPMS, and an enhancement of Val content. A higher activity of AHAS could also raise the levels of Ile, but this does not occur probably due to feedback inhibition by Ile of Thr dehydratase—the enzyme that makes 2-oxobutyrates, the substrate of AHAS for Ile synthesis (Singh, 1999; Coruzzi and Last, 2000).

#### *IPMS1* and *IPMS2* Differ Somewhat in Gene Expression Pattern and Properties of the Encoded Protein

Based on RT-PCR analyses and publicly available microarray experiments assembled with the

GENEVESTIGATOR program (Supplemental Figs. S4 and S5), both *IPMS* genes are constitutively expressed throughout the plant and thus can complement each other, consistent with the normal Leu phenotype of the insertion mutant lines. However, the two genes are at least subfunctionalized at a regulatory level (Moore and Purugganan, 2005) since *IPMS1* expression, but not that of *IPMS2*, is twice as high in seeds as in most other plant tissues. In the developing seed, Leu is one of the main free amino acids and may be specifically synthesized there since it is not abundant in the phloem (Baud et al., 2002). The particular role of *IPMS1* during seed development might explain the 20% reduction in seed fecundity reported by Field et al. (2004) for an *IPMS1* knockout line.

The major biochemical difference between *IPMS1* and *IPMS2* appears to be the  $K_m$  value for acetyl-CoA, 45  $\mu\text{M}$  and 16  $\mu\text{M}$ , respectively, making *IPMS2* the more efficient enzyme at comparable turnover numbers. Calibrated gel-filtration chromatography showed that *IPMS1* is active as a dimer (124 kD), whereas *IPMS2* is mainly active as a tetramer (approximately 280 kD; Fig. 4C); nonetheless, these data should be interpreted with care as both proteins contain a His-tag that might influence the formation of quaternary structure (Wu and Filutowicz, 1999). The *IPMS* enzymes previously isolated from microorganisms were characterized either as dimers (*Saccharomyces cerevisiae*, *Corynebacterium glutamicum*, *Mycobacterium tuberculosis*) or tetramers (*Salmonella typhimurium*; Leary and Kohlhaw, 1972; Roeder and Kohlhaw, 1980; Pátek et al., 1994; Koon et al., 2004). Gel filtration of the *IPMS* activity present in crude extracts of *Arabidopsis* showed a broad band of enzyme activity between 50 and 200 kD with a major peak at 95 to 120 kD (Textor et al., 2004). Assuming that *IPMS1* is also present as a dimer in vivo and *IPMS2* mostly as a tetramer, the main *IPMS* activity present in the plant crude extract is *IPMS1*.

#### Other *IPMS*s Have Different Kinetic Constants, Cation Preferences, and Sensitivity to Leu Feedback Inhibition

The  $K_m$  of *IPMS1* and *IPMS2* for 2-oxoisovalerate are similar to each other (304  $\mu\text{M}$  and 279  $\mu\text{M}$ ) and are much higher than the reported value of 75  $\mu\text{M}$  for the *IPMS* present in spinach chloroplasts. The spinach *IPMS* also has a distinct  $K_m$  value for acetyl-CoA, 5  $\mu\text{M}$  versus 45  $\mu\text{M}$  and 16  $\mu\text{M}$  for *IPMS1* and *IPMS2*, respectively (Hagelstein and Schultz, 1993).

The *IPMS* enzymes of *Arabidopsis*, just as the spinach *IPMS*, are dependent upon millimolar concentrations of  $\text{Mg}^{2+}$  (Fig. 4) for optimal enzyme activity. This cofactor can only be replaced with  $\text{Mn}^{2+}$ , which yields about 50% of the initial enzyme activity. However,  $\text{Mn}^{2+}$  is clearly preferred over  $\text{Mg}^{2+}$  as a cofactor by the MAM enzymes (Falk et al., 2004; Textor et al., 2004). Some *IPMS* enzymes of fungi and bacteria also employ  $\text{Mn}^{2+}$  or  $\text{Zn}^{2+}$  as a cofactor (Stieglitz and Calvo, 1974; Wiegel, 1978; Roeder and Kohlhaw, 1980; Koon et al., 2004). The broad pH optima at 8.5 obtained for *IPMS1*

and *IPMS2* is common for *IPMS*s, irrespective of their source, and the same pH dependence has also been observed for the MAMs (Falk et al., 2004; Textor et al., 2004).

Generally, enzymes at critical branchpoints in plant amino acid biosynthesis are feedback inhibited by their end-product amino acids (Coruzzi and Last, 2000). Accordingly, Leu inhibits the enzyme activity of both heterologously expressed *IPMS*s. A maximum of 30% to 35% inhibition was reached around a concentration of 1 mM Leu (Fig. 5), and a similar effect was detected on the *IPMS* activity in the crude extract of *Arabidopsis*. A somewhat greater effect has been reported on the *IPMS* present in crude extracts of maize embryos (61% inhibition at 50  $\mu\text{M}$  Leu, 84% inhibition at 5 mM Leu; Oaks, 1965), but the *IPMS* of spinach chloroplasts was reported to be 100% inhibited by micromolar concentrations of Leu (Hagelstein and Schultz, 1993). However, in a chloroplast-enriched crude extract from spinach, we only detected a 66% inhibition of *IPMS* at 5 mM Leu. A 100% inhibition of *IPMS* activity at 1 mM concentrations of Leu is common among bacteria (Stieglitz and Calvo, 1974). The production of 2-oxoisovalerate itself is regulated through feedback inhibition of AHAS by Leu, Val, and Ile (Fig. 1; Singh, 1999). Concentrations of 1 to 5 mM of these amino acids result in a 45% to 65% inhibition of AHAS enzyme activity in *Arabidopsis* (Lee and Duggleby, 2001) and other plants (Mifflin and Cave, 1972), i.e. an effect of similar magnitude as that of 1 to 5 mM Leu on *IPMS* activity.

#### *IPMS*s Produce Other Products in Vitro and in Vivo

The substrate specificity of *IPMS*s is not very high. For example, the reported reaction rates for 2-oxobutyrate are usually higher than those found for the true substrate 2-oxoisovalerate, despite the higher  $K_m$  for 2-oxobutyrate (Webster and Gross, 1965; Strassman and Ceci, 1967; Rabin et al., 1968; Gross, 1970; Kohlhaw and Leary, 1970; Ulm et al., 1972; Wiegel and Schlegel, 1977; Wiegel, 1981; Kohlhaw, 1988). This is also true for the *Arabidopsis* enzymes. In addition, most reported *IPMS*s and, to a lesser extent, the MAMs from *Arabidopsis* (S. Textor, unpublished data) can catalyze the condensation between pyruvate and acetyl-CoA. The product of this condensation reaction, citramalate, has been reported as a metabolite in *Arabidopsis* (Fiehn et al., 2000) and tomato (27.6  $\mu\text{mol g}^{-1}$  fresh weight in orange-colored fruits; Roessner-Tunali et al., 2003). The presence of citramalate has led to the suggestion that plants possess a tricarboxylic acid cycle bypass previously described in bacteria (Grant and Smith, 2000). Citramalate may also have a function in Ile biosynthesis by serving as a precursor of 2-oxobutyrate, a substrate for AHAS. This metabolic route has been demonstrated for a mutant of the microorganism *Serratia marcescens* (Kisumi et al., 1977), the halophilic archaeon *Haloarcula hispanica* (Hochuli et al., 1999), and in *Leptospira interrogans* (Xu et al., 2004).

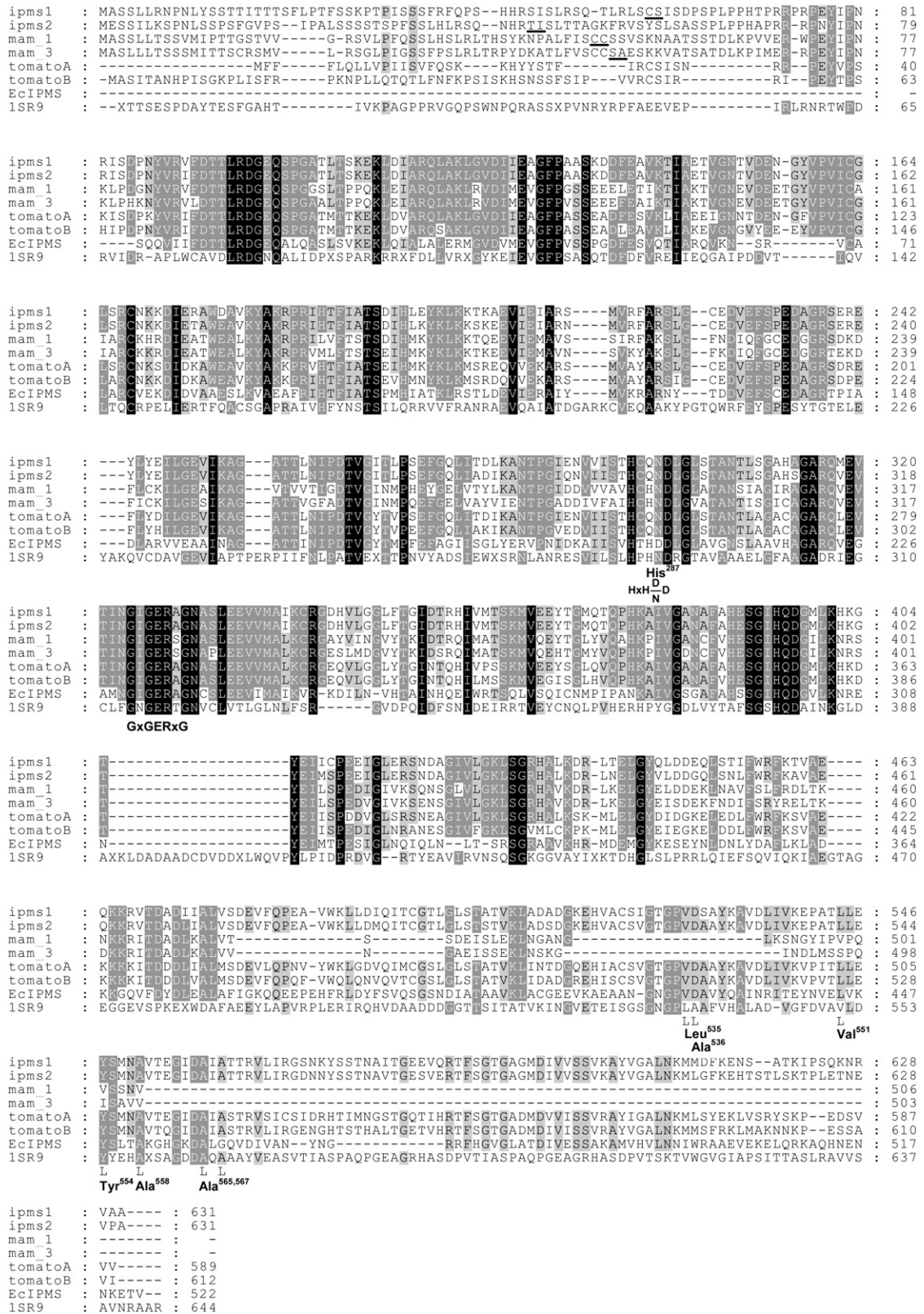


**Figure 8.** Alignment of deduced amino acid sequences for IPMS1, IPMS2, MAM1, and MAM3 with IPMS sequences from wild tomato (GenBank accession nos. AAB61598 and AAB61599), *E. coli* (Swiss-Prot: P09151), and *M. tuberculosis* whose protein structure has been elucidated (PDB: 1SR9). Black shading indicates individual amino acids that are conserved within all sequences, dark gray shading individual amino acids that are identical in at least six out of eight sequences, and light gray

Compounds with a carbon chain length longer than 2-oxoisovalerate, like 2-oxovalerate, 4-methyl-2-oxovalerate, and 2-oxohexanoate, have usually been reported to be active-site inhibitors of IPMS (Webster and Gross, 1965; Gross, 1970; Kohlhaw and Leary, 1970; Ulm et al., 1972; Wiegel and Schlegel, 1977; Wiegel, 1981; Kohlhaw, 1988) rather than substrates, as described in this study. An exception is the paper of Rabin et al. (1968) that reports on the conversion of 2-oxovalerate, 4-methyl-2-oxovalerate, and 2-oxohexanoate by an IPMS activity from *Pseudomonas aeruginosa* at yields comparable to those reported here. Our results indicate that the IPMSs from Arabidopsis and *E. coli* can use 2-oxo acids ranging in length from glyoxylate to 2-oxohexanoate. However, the shortest and longest substrates react at rates that might have escaped detection in older work with less-sensitive methods.

### IPMS and MAM Proteins Share Some But Not All Structural Features

The most striking difference between the amino acid sequences of the IPMS and MAM proteins from Arabidopsis is the absence of about 150 amino acids at the C-terminal domain of the MAMs (Fig. 8). This domain contains a conserved allosteric Leu binding site (Koon et al., 2004) whose absence is likely responsible for the lack of Leu inhibition of the *E. sativa* MAM synthase (Falk et al., 2004). One can expect the MAMs of Arabidopsis to show similar behavior. The only published crystal structure for an IPMS is that of the *M. tuberculosis* protein (Koon et al., 2004). Although Arabidopsis IPMS1 and IPMS2 share only about 25% amino acid identity with the *M. tuberculosis* protein (Fig. 8; 1SR9), the amino acids of the hydrophobic Leu binding pocket of the *M. tuberculosis* protein are either conserved in the Arabidopsis proteins (Tyr-554, Ala-558, Ala-565, Ala-567) or replaced by comparable amino acids (Leu-535 → Val, Val-551 → Ala), except for Ala-536, which is substituted by the more hydrophilic Asp. All of the amino acid residues of the *M. tuberculosis* IPMS involved in binding acetyl-CoA and 2-oxoisovalerate, including the GxGERxG motif, are conserved in the IPMS and MAM sequences of Arabidopsis. However, the HxH(D/N)D motif involved in binding of the metal ion is less conserved. The second His residue (His-287) is substituted by Gln in the IPMS sequences of Arabidopsis and wild tomato (but not in the MAM sequences), and there is a substitution of Ala by Ser, six amino acid residues upstream. Such changes might explain why the Arabidopsis IPMSs use Mg<sup>2+</sup> as cofactor instead of Zn<sup>2+</sup> as

the *M. tuberculosis* IPMS does. The cofactor Zn<sup>2+</sup> preferably binds to nitrogen and sulfur-containing amino acid side chains, such as those of His, while Mg<sup>2+</sup> prefers residues with oxygen functions (such as the carbonyl group of Gln and hydroxyl group of Ser). The favored cofactor of the MAM proteins, Mn<sup>2+</sup>, behaves similarly as Mg<sup>2+</sup> but nonetheless has higher affinity with nitrogen-containing ligands than Mg<sup>2+</sup> (Bock et al., 1999; Glusker et al., 1999).

Apart from their 60% similarity in amino acid sequence, the close similarity between the IPMSs and the MAMs of Arabidopsis can also be deduced from their overlapping substrate specificities. The IPMSs are able to catalyze the condensation reaction with the MAM substrate 4-methylthio-2-oxobutyrate (Table II). Conversely, purified MAM3 can catalyze the reaction with 2-oxoisovalerate (S. Textor, unpublished data), even though both of these reactions occur at such low rates that they probably do not play a major role in planta. In this respect, it is remarkable that ectopic overexpression of a presumptive IPMS from *B. atlantica* (*BatIMS*) in Arabidopsis caused a doubling of aliphatic glucosinolates in the leaves of the T<sub>1</sub> generation in addition to perturbed amino acid levels (Field et al., 2006). However, these changes seem unlikely to be the result of an overlap in substrate specificity between IPMS and MAM, since this transformant displayed extensive morphological, metabolic, and transcriptional changes, including the up-regulation of at least four of the 10 known genes of the aliphatic glucosinolate biosynthetic pathway.

The ability to catalyze a reaction with 4-methylthio-2-oxobutyrate at a very low rate is not restricted to the IPMSs of glucosinolate-producing plants like Arabidopsis, but is also characteristic of the IPMS of *E. coli* (Supplemental Fig. S1), suggesting that it is an inherent property of this enzyme type. This overlap in substrate usage plus the approximate 60% amino acid identity between IPMSs and MAMs makes it plausible that MAMs were derived from an ancestral IPMS through gene duplication. Such duplication could have persisted if it had no negative effects on Leu homeostasis. Post-transcriptional mechanisms like Leu inhibition of IPMS activity may ensure that there are no major changes in amino acid content despite changes in IPMS gene expression, as seen in the case of the *IPMS1* and *IPMS2* mutants. Subsequent neofunctionalization (Moore and Purugganan, 2005) of one of the IPMS duplicate copies to a MAM would have involved selection for an increase in substrate specificity toward 4-methylthio-2-oxobutyrate and the loss of the regulatory domain for Leu feedback inhibition at some stage in this process. Either as a consequence of these changes or through

#### Figure 8. (Continued.)

shading amino acids that are identical in at least five out of eight sequences. The ChloroP-predicted cleavage sites are marked with an underscore. Amino acid residues mentioned in the text are represented below the alignment, likewise amino acid residues of the Leu binding site that are marked with an "L" and the conserved motifs GxGERxG and HxH(D/N)D. Amino acid positions are numbered relative to 1SR9.

additional selection, most of the original activity for 2-oxoisovalerate has been lost and some of the MAMs have developed affinities for substrates even larger than 4-methylthio-2-oxobutyrate. In future research, we will seek evidence for this scenario and try to determine what structural changes in IPMS accompanied this process.

## MATERIALS AND METHODS

### Plants

Seeds of Arabidopsis (*Arabidopsis thaliana* L. Heynh), ecotype Col-0 (CS3879 Arabidopsis Biological Resource Center), were sown densely in ordinary potting soil mixed with vermiculite (3:1). Plants were raised in a controlled growth chamber with a diurnal cycle of 10 h light and 14 h dark at 22°C. Illumination was from a mixture of Fluora (Osram) and Cool White lamps at  $230 \mu\text{mol m}^{-2} \text{s}^{-1}$ . Seeds of the Salk mutant lines were obtained from the European Arabidopsis Stock Centre (Nottingham, UK).

### RNA Isolation and cDNA Cloning

Total RNA was isolated from liquid nitrogen-frozen root tissue (*IPSM1*) or total leaf tissue (*IPMS2*) with Trizol reagent (Invitrogen) according to manufacturer's instructions. First-strand cDNA was synthesized with 2  $\mu\text{g}$  of total RNA, 200 units of MMLV reverse transcriptase (Promega), and 0.5  $\mu\text{g}$  of gene-specific oligonucleotide primer using the reagents and instructions provided.

*IPMS2* was amplified from the first-strand cDNA product using the primer pair *lipms2m/2ipms2n* (for all primers used, see Supplemental Table S1), resulting in a truncated *ORF* lacking 138 nucleotides corresponding to a putative chloroplast transit peptide (ChloroP; Emanuelsson et al., 1999). The reaction product was gel purified using a QiaQuick gel extraction kit (Qiagen), cloned directly into the pBAD-TOPO (Invitrogen) expression vector, and transformed into TOP10 cells (Invitrogen) according to the manufacturer's instructions. The DNA of transformed colonies was purified by a miniprep (Invisorb spin plasmid mini kit; Invitex) and screened by restriction analyses and DNA sequencing on an ABI 3700 DNA sequencer with Big Dye terminators (PE Applied Biosystems).

As protein expression of the *IPMS2/pBAD-TOPO* construct in BL21-Codon-Plus-RIL cells (Stratagene) was very poor, *IPMS2* was subcloned into the pCR-T7/CT-TOPO vector (Invitrogen). The desired *IPMS2* fragment was obtained from the previous *IPMS2/pBAD-TOPO* construct in a PCR reaction using the Expand High Fidelity PCR system (La Roche) and the primer pair *lipms2m+atg/2ipms2n* in accordance with the provided instructions. The PCR fragment produced was directly cloned into the pCR-T7/CT-TOPO vector and transformed into TOP10F' *Escherichia coli* cells. The resulting bacterial colonies were screened for presence of the desired *IPMS2/pCR-T7/CT-TOPO* construct.

A cDNA corresponding to the entire ORF of *IPMS1* was amplified from the first-strand product using the primer pair *lipms1k/2ipms1j* in a PCR with Pfu-Turbo DNA polymerase (Stratagene). The reaction product was gel purified, cloned directly into the pCR4-TOPO (Invitrogen) vector, and transformed into TOP10 *E. coli* cells (Invitrogen). Screening for the desired *IPMS1/pCR4-TOPO* construct yielded a construct that had a single C-to-T mutation at position 176. This mutation was corrected by use of primer *lipms1i+atg* that together with primer *2ipms1j* was used to amplify *IPMS1* without the 171 nucleotides coding for a putative ChloroP-predicted chloroplast transit peptide. The PCR product obtained from the Expand High Fidelity PCR system was directly cloned into the pCR-T7/CT-TOPO vector and transformed into TOP10F' *E. coli* cells. However, none of the clones contained an *IPMS1/pCR-T7/CT-TOPO* construct that was free of point mutations. We attempted to restore a construct that had only one point mutation at nucleotide 169 with the QuickChange site-directed mutagenesis kit of Stratagene using primers *mut1-for* and *mut1-for-r*. An *IPMS1/pCR-T7/CT-TOPO* construct was isolated that had a single—though silent—point mutation at nucleotide position 169 of the truncated cDNA (codon GAC changed into GAT).

### cDNA Expression in *E. coli*

The *IPMS1/pCR-T7/CT-TOPO* construct and *IPMS2/pBAD-TOPO* construct were both expressed in *E. coli* strain BL21(DE3) pLysS (Invitrogen). A

fresh colony harboring the construct was picked from the plate with a sterile toothpick and grown on 25 mL of Luria-Bertani medium with chloramphenicol (34  $\mu\text{g}/\text{mL}$ ) and ampicillin (100  $\mu\text{g}/\text{mL}$ ) for 62 h at 18°C. This 25 mL of culture was used to inoculate another 500 mL of antibiotic-containing medium (2 × 250 mL) that was subsequently incubated at 18°C until an  $\text{OD}_{600}$  of 0.6 was reached. Expression of the cDNA was then induced with 2 mM IPTG and incubation continued overnight. Cells were harvested the next morning by centrifugation in 50 mL Falcon tubes for 10 min at 6,500g and 4°C, and the bacterial pellets were stored at -80°C.

### Purification of the Expressed His-Tag Protein

A bacterial pellet was homogenized in a 2-mL Eppendorf tube with 1.5 mL of lysis buffer, containing 50 mM sodium borate buffer, pH 8.0, 300 mM NaCl, 10 mM imidazole, and 1 mM  $\text{MgCl}_2$ , and left on ice for 30 min after the addition of  $1.0 \times 10^5$  units lysozyme (Merck). A few glass beads ( $\varnothing$  2 mm) were put in the tube and the cells were disrupted in a sonicator bath (Sonorex RK100, 35 kHz; Bandelin) filled with ice water ( $3-4 \times$ , 3 min). Cell debris was precipitated by centrifugation for 7 min at 20,500g and 4°C.

A Poly-Prep chromatography column (2-mL bed volume, 10-mL reservoir; Bio-Rad) was prepared with 1.5 mL of 50% Ni-NTA agarose (Qiagen) and rinsed with 5 mL of lysis buffer. The bacterial lysate was added to the resin and the column was placed on a rotator for 1 h at 4°C, allowing the His-tag protein to bind to the resin. The column was then placed in a vertical position and washed with 12 mL of wash buffer, which had the same composition as lysis buffer except for an elevated (20 mM) concentration of imidazole. The His-tag protein was eluted with 3 mL of buffer containing 250 mM imidazole, and the eluent was immediately transferred to an Econo-Pac 10 DG column (Bio-Rad) and desalted into 4 mL of a 50 mM Tris buffer, pH 8.0, containing 1 mM  $\text{MgCl}_2$  and 10% glycerol. This desalted preparation was used for enzyme assays. The protein concentration of each preparation was determined with the BCA protein assay kit (Pierce) using bovine serum albumin as a standard; concentrations generally ranged from 300 to 600  $\mu\text{g}/\text{mL}$ .

### Enzyme Assays

#### Qualitative Assay Using Radio-HPLC Detection

The assay contained 100  $\mu\text{L}$  of enzyme preparation that was incubated at 30°C with 3 mM of the 2-oxo-acid substrate, 500  $\mu\text{M}$  [ $1-^{14}\text{C}$ ]acetyl-CoA (from Hartmann, diluted with unlabeled acetyl-CoA [Sigma-Aldrich] to 0.4 mCi  $\text{mmol}^{-1}$ ) and 4 mM  $\text{MgCl}_2$ , in a final volume of 250  $\mu\text{L}$  100 mM Tris buffer, pH 8.0. The incubation was stopped after 1 h by adding 750  $\mu\text{L}$  ethanol. The denatured protein was precipitated by centrifugation and the supernatant reduced to a volume of approximately 100  $\mu\text{L}$  using a DNA Speedvac 1100 (Savant). A portion of the concentrated supernatant (20  $\mu\text{L}$ ) was analyzed on the radio-HPLC according to Falk et al. (2004).

#### Continuous Spectrophotometric Assay (NEM Assay)

The reaction mixture contained 10 to 500  $\mu\text{M}$  acetyl-CoA, 50 to 2,000  $\mu\text{M}$  2-oxoisovalerate, 0.1 mM NEM (Sigma-Aldrich), 4 mM  $\text{MgCl}_2$ , 100 mM Tris, pH 8.0, and 5  $\mu\text{L}$  of enzyme preparation in a total volume of 500  $\mu\text{L}$ . The change in optical density over time at 30°C was followed against a solution of 1 mM NEM in a UV-2501PC spectrophotometer (Shimadzu) using micro quartz cuvettes (Hellma) with black walls. The loss of the thioesterbond in acetyl-CoA and the loss of a double bond in NEM upon binding to CoA-SH result in an  $\text{AOD}_{232}$  of  $-1.08 \times 10^4$  (1-cm light path) per mole of CoA-SH formed (Webster and Gross, 1965).

#### Spectrophotometric End-Point Assay (DTNB Assay)

The enzyme preparation (1–5  $\mu\text{L}$ ) was incubated for 10 min at 30°C with 10 mM 2-oxoisovalerate, 500  $\mu\text{M}$  acetyl-CoA, 4 mM  $\text{MgCl}_2$ , and 100 mM Tris, pH 8.0, in a total volume of 150  $\mu\text{L}$ . Incubations were synchronized by pipetting the enzyme solution in the lid of an Eppendorf tube containing the incubation mixture, after which the enzyme in all vessels was simultaneously spun down for a few seconds in a table-top centrifuge; reactions were stopped by freezing the vessels in liquid nitrogen. To the frozen reaction mixture, 200  $\mu\text{L}$  of ethanol and 200  $\mu\text{L}$  of a fresh 1 mM solution of DTNB (Sigma-Aldrich) in 100 mM Tris, pH 8.0, were added. The mixture was left at room temperature to allow the

free thiol group of CoA to react with DNTB, forming a yellow-colored, 3-carboxy-4-nitrothiophenol anion with an  $\epsilon_{412}$  of  $14,140 \text{ M}^{-1} \text{ cm}^{-1}$  (Kohlhau, 1988). When no further color developed, the mixture was centrifuged for 5 min at  $16,000g$  and the absorbance measured against water at 412 nm. The enzyme assay was corrected for unspecific hydrolysis of acetyl-CoA by subtracting the absorbance of a blank incubation where no 2-oxo-acid substrate had been added. The assay was generally linear for the first 15 min with  $2 \mu\text{g}$  of protein.

## Enzyme Characterization

### Substrate Specificity

The various 2-oxo acid substrates tested in the radio-HPLC assay with [ $^{14}\text{C}$ ]acetyl-CoA were either obtained from Fluka or Sigma-Aldrich, or synthesized in our laboratories (Falk et al., 2004; S. Textor, unpublished data). Reaction rates of the different substrates were determined at 20 mM (estimated to be a saturating concentration) with the DNTB assay; the amount of enzyme added was varied from 1 to  $50 \mu\text{L}$ , depending on the substrate, to stay within detection limits.

### Enzyme Kinetics

The  $K_m$  and  $V_{\max}$  values for acetyl-CoA and 2-oxo-isovalerate were determined with the NEM assay. They were calculated from the recorded initial (linear) reaction rates at different substrate concentrations of three to four independent experiments using the Enzyme Kinetic Module (Version 1.1) of Sigmaplot (Version 8.0).

### Other Enzyme Characteristics

The pH optima for IPMS1 and IPMS2 were determined in the pH range of 5.5 to 10.5 in 0.5-pH units using the DTNB assay in which Tris buffer was replaced by MES (pH 5.5–6.5), BisTris-propane (pH 6.5–9.5), or 2-amino-2-methyl-1-propanol (pH 9.5–10.5). The DTNB assay was also used to test the effect of Leu on enzyme activity in a range from  $25 \mu\text{M}$  to 10 mM. Furthermore, the effect on enzyme activity of  $\text{Mg}^{2+}$  concentration,  $\text{Mn}^{2+}$ , and  $\text{K}^+$  was investigated with the DTNB assay taking an enzyme preparation after His-tag purification that had been desalted to Tris buffer lacking  $\text{MgCl}_2$ . The effect of other cations, i.e.  $\text{Ca}^{2+}$ ,  $\text{Co}^{2+}$ ,  $\text{Cu}^{2+}$ ,  $\text{Fe}^{2+}$ ,  $\text{K}^+$ ,  $\text{Mn}^{2+}$ , and  $\text{Zn}^{2+}$ , on this enzyme preparation had to be tested with the qualitative radio-HPLC assay because these ions are strong oxidizers that react with the 3-carboxy-4-nitrothiophenol anion of the DNTB assay, causing a rapid loss of the yellow color. All cations were used as their chloride salts, except  $\text{Fe}^{2+}$  and  $\text{Zn}^{2+}$  that were used as their sulfate salts.

The molecular mass of the native recombinant protein was estimated by exclusion chromatography on a Superdex 200 column (Hiload 16/60; Pharmacia Biotech) that had been calibrated with  $\beta$ -amylase (200 kD), alcohol dehydrogenase (150 kD), bovine serum albumin (66 kD), carbonic anhydrase (29 kD), and cytochrome C (12.4 kD). The column was loaded with  $200 \mu\text{L}$  of enzyme preparation and eluted at  $1 \text{ mL min}^{-1}$  with a buffer consisting of 50 mM Tris, pH 8.0, 10% glycerol, and 150 mM NaCl. Sixty fractions of 1 mL were collected after discarding the first 40 mL of eluent, and  $138.5 \mu\text{L}$  of each fraction was tested in a modified DNTB assay (25-min incubation at room temperature) for enzyme activity.

## *E. coli* CV512 Complementation and Origin of *E. coli* IPMS

The IPMS1/pCR-T7/CT-TOPO and IPMS2/pBAD-TOPO cDNA constructs were transformed in *E. coli* CV512 ( $\text{F}^+$  leuY371; Somers et al., 1973). The CV512 strain lacks functional IPMS and is able to grow on M9 minimal medium with Glc as a carbon source only when it is either supplemented with Casamino acids (Difco) or transformed with a construct containing a functional IPMS. To ensure expression from a T7 polymerase-driven construct, the IPTG inducible T7-polymerase gene was introduced into strain CV512 by a  $\lambda\text{DE3}$  lysogenation kit (Novagen) giving CV512(DE3). As a positive control, a pET28a (Novagen) construct harboring the *E. coli* DH5 $\alpha$  (Hanahan, 1983) IPMS gene *leuA* was used for complementation studies. The *leuA* gene was amplified by PCR from DH5 $\alpha$  with the primer pair IPMFEff/IPMErv (Supplemental Table S1) and cloned into pET28a using the *Bam*HI/*Xho*I restriction sites provided

by the primers. Complementation efficiency was tested at two different incubation temperatures,  $30^\circ\text{C}$  and  $37^\circ\text{C}$ .

The pET28a/LeuA construct was also used as a source of *E. coli* IPMS that was tested in the radio-HPLC assay for its substrate specificity. BL21(DE3) *E. coli* cells (Invitrogen) with the LeuA construct were grown in 100 mL of Luria-Bertani medium containing  $50 \mu\text{g mL}^{-1}$  kanamycin at  $37^\circ\text{C}$  until an  $\text{OD}_{600}$  of 0.5 was reached. Expression was induced with 1 mM IPTG and incubation continued for 2.5 h. Cells were harvested and the expressed protein isolated and purified in the same way as described for the Arabidopsis IPMSs, taking advantage of the C-terminal His-tag present in the construct.

## Plant Mutant Lines

### PCR of Genomic DNA

Genomic DNA was extracted from expanding leaves using an abbreviated protocol of Rogers and Bendich (1985). About 5 mg of young leaf tissue was collected in a 1.5-mL microfuge tube and homogenized with  $10 \mu\text{L}$  of  $2\times$  CTAB solution (2% cetyltrimethylammonium bromide [w/v], 100 mM Tris, pH 8.0, 1.4 M NaCl, 1% polyvinylpyrrolidone [4,000 molecular weight]) using a micropestle. The sample was incubated at  $65^\circ\text{C}$  for 1 to 2 min, cooled briefly on ice, and extracted with  $10 \mu\text{L}$  of chloroform:isoamyl alcohol (24:1, v/v). After  $10 \mu\text{L}$  of water was added, the samples were subjected to centrifugation at  $11,000g$ . The upper phase was recovered and 0.1 to  $0.5 \mu\text{L}$  was used per PCR of  $20\text{-}\mu\text{L}$  volume (for details, see below).

### PCR of RNA Transcript

Total RNA was isolated from freshly harvested, freeze-dried whole rosettes of individual 3- to 4-week-old plants with Trizol reagent (Invitrogen) according to the manufacturer's instructions. A cDNA population was synthesized with  $2 \mu\text{g}$  of RNA, either  $0.5 \mu\text{g}$  of  $\text{dT}_{12-18}$  or  $0.17 \mu\text{g}$  of gene-specific primers (Invitrogen) and 200 units of MMLV reverse transcriptase (Promega) using the reagents and instructions provided. From each of these reverse transcriptase reactions, a  $20\text{-}\mu\text{L}$  PCR was prepared consisting of  $1\times$  PCR buffer (Promega), 0.2 mM dNTPs,  $0.5 \mu\text{M}$  each primer (see Supplemental Table S1 for specific primer pairs for *ACT8*, *IPMS1*, and *IPMS2*), 0.5 units of Taq Polymerase (Promega), and an aliquot of reverse transcriptase reaction equivalent to 40 ng of template RNA. The reactions were subjected to an initial thermal denaturation of  $94^\circ\text{C}$  for 2 min, followed by 30 or 35 cycles at  $94^\circ\text{C}$  for 30 s, a primer-dependent annealing temperature for 30 s,  $72^\circ\text{C}$  for 2 min, and a final incubation at  $72^\circ\text{C}$  for 5 min. After electrophoresis and incubation in ethidium bromide, DNA fragments were analyzed and quantified (GeneGenius with GeneTools Analysis Software Version 3.02 [Synoptics]; or Gel Logic 200 with Kodak MI software). PCRs of each individual reverse transcriptase reaction with specific oligonucleotide primer pairs were done at least two times.

### Amino Acid Analyses

The procedure was optimized to extract total free amino acids from Arabidopsis plant material and to quantify the individual amino acids in a single HPLC run. The amino acids present in a crude plant extract were derivatized with mercaptoethanol and *O*-phthalaldehyde yielding a fluorescent isoindole (Roth, 1971; Sarwar and Botting, 1993), a method inappropriate for the detection of Cys (weakly fluorescent derivative) and Pro (contains no primary amino group for derivatization reaction). Rosettes of individual 3- to 4-week-old individual plants were harvested, and individually frozen in liquid nitrogen, lyophilized, and pulverized. Aliquots of 10 and 50 mg were transferred to 2-mL Eppendorf tubes and resuspended with  $0.8 \text{ mL}$  of 0.1 N HCl to rehydrate the tissue. After incubation for 15 min at room temperature, the samples were centrifuged at  $16,000g$  and the supernatant transferred to a fresh tube. Samples for HPLC were prepared by adding  $50 \mu\text{L}$  of the supernatant to a  $350\text{-}\mu\text{L}$  glass vial insert containing  $50 \mu\text{L}$  of a 1:1 (v/v) solution of 0.1 N HCl and 0.5 M potassium borate, after which the vials were capped. The autosampler of the HPLC (Agilent HP1100 series) was programmed to mix the vial content with  $30 \mu\text{L}$  of reagent consisting of 0.085 M *O*-phthalaldehyde (Fluka) and 1% (v/v)  $\beta$ -mercaptoethanol in a 0.5 M sodium borate solution immediately before injection of  $50 \mu\text{L}$  of sample onto the HPLC column (Supelcosil LC-18-DB [ $250 \times 4.6 \text{ mm}$ ,  $5\text{-}\mu\text{m}$  particle size]; Supelco). The column was run with a 0.02 M citrate solution of pH 5.5 (solvent A) and methanol:acetonitrile (65:35, v/v; solvent B) at  $28^\circ\text{C}$  with a gradient as follows: 15% of solvent B at start, linear gradient to 38.5% of



solvent B over 42 min, increase to 45% of solvent B in 1 min, linear gradient to 62.5% of solvent B over 20 min, increase to 100% of solvent B in 0.5 min, 100% of solvent B for 3 min, decrease to 15% of B in 0.5 min, and re-equilibration of the column at 15% of solvent B for 8 min (total time of run is 75 min). The derivatized amino acids were measured with a fluorescence detector (Agilent HP1100 series) at an excitation wavelength of 340 nm and an emission wavelength of 445 nm. Amino acid samples were quantified by calibration curves that were prepared with a 0.5 mM amino acid stock solution of Asn, His, and Gln and an amino acid stock solution of Fluka that contained all the other amino acids in a 0.5 mM concentration. Aliquots of 5, 10, 20, 30, 40, and 50  $\mu$ L amino acid standard solution were added to a 350- $\mu$ L glass vial insert and adjusted to 50  $\mu$ L with 0.1 N HCl. The vials were capped after the addition of 50  $\mu$ L of 0.5 M potassium borate and run in the same sequence as the plant samples.

### Glucosinolate Analyses

Glucosinolates were extracted from 10 mg of lyophilized plant material and converted into their desulfoglucosinolate counterparts according to Brown et al. (2003). The desulfoglucosinolates were identified and quantified by HPLC analyses on a C18 reversed-phase column (LiChrospher RP-18, 250  $\times$  4.6 mm i.d., 5- $\mu$ m particle size; Chrompack) by comparison of retention times and UV spectra to those of purified standards and by measuring the  $A_{229}$  relative to an internal standard (Reichelt et al., 2002; Brown et al., 2003).

### Supplemental Data

The following materials are available in the online version of this article.

**Supplemental Figure S1.** Radio-HPLC analyses of the biochemical assay for the IPMS of *E. coli*.

**Supplemental Figure S2.** Predicted positions of the T-DNA inserts in the Salk knockout lines for *IPMS1* (Salk\_101771) and *IPMS2* (Salk\_051060 and Salk\_000074).

**Supplemental Figure S3.** Analyses of the glucosinolate content of homozygotic T-DNA insertion lines for *IPMS1* (Salk\_101771 [mm]) and *IPMS2* (Salk\_051060 [mm] and Salk\_000074 [mm]).

**Supplemental Figure S4.** Semiquantitative RT-PCR analysis of *IPMS1* and *IPMS2* gene expression in various plant organs.

**Supplemental Figure S5.** Expression levels of *IPMS1* and *IPMS2* in different plant tissues and various growth stages according GENEVESTIGATOR.

**Supplemental Table S1.** Oligonucleotide primers used in this study.

### ACKNOWLEDGMENTS

We thank Axel Schmidt for his advice on cloning and expression procedures, Kimberly Falk for her help and advice in the isolation of IPMS activities from crude plant extracts, and Michael Reichelt for his assistance with the HPLC analyses. We thank the Arabidopsis Biological Resource Center and the Nottingham Arabidopsis Stock Centre for providing Arabidopsis plant lines.

Received June 21, 2006; accepted December 7, 2006; published December 22, 2006.

### LITERATURE CITED

- Alonso JM, Stepanova AN, Leisse TJ, Kim CJ, Chen H, Shinn P, Stevenson DK, Zimmerman J, Barajas P, Cheuk R, et al (2003) Genome-wide insertional mutagenesis of *Arabidopsis thaliana*. *Science* **301**: 653–657
- Baud S, Boutin J-P, Miquel M, Lepiniec L, Rochat C (2002) An integrated overview of seed development in *Arabidopsis thaliana* ecotype WS. *Plant Physiol Biochem* **40**: 151–160
- Bock CW, Katz AK, Markham GD, Glusker JP (1999) Manganese, a replacement for magnesium and zinc: functional comparison of the divalent ions. *J Am Chem Soc* **121**: 7360–7372

- Brown PD, Tokuhsa JG, Reichelt M, Gershenzon J (2003) Variation of glucosinolate accumulation among different organs and developmental stages of *Arabidopsis thaliana*. *Phytochemistry* **62**: 471–481
- Campos de Quiros H, Magrath R, McCallum D, Kroymann J, Schnabelrauch D, Mitchell-Olds T, Mithen R (2000)  $\alpha$ -Keto acid elongation and glucosinolate biosynthesis in *Arabidopsis thaliana*. *Theor Appl Genet* **101**: 429–437
- Chisholm MD, Wetter LR (1964) Biosynthesis of mustard oil glucosides. IV: the administration of methionine- $C^{14}$  and related compounds to horseradish. *Can J Biochem* **12**: 1033–1040
- Coruzzi G, Last R (2000) Amino acids. In B Buchanan, W Gruissem, R Jones, eds, *Biochemistry and Molecular Biology of Plants*. American Society of Plant Physiologists, Rockville, MD, pp 358–411
- Ellerstrom M, Josefsson LG, Rask L, Ronne H (1992) Cloning of a cDNA for rape chloroplast 3-isopropylmalate dehydrogenase by genetic complementation in yeast. *Plant Mol Biol* **18**: 557–566
- Emanuelsson O, Nielsen H, von Heijne G (1999) ChloroP, a neutral network-based method for predicting chloroplast transit peptides and their cleavage sites. *Protein Sci* **8**: 978–984
- Falk KE, Vogel C, Textor S, Bartram S, Hick A, Pickett JA, Gershenzon J (2004) Glucosinolate biosynthesis: demonstration and characterization of the condensing enzyme of the chain elongation cycle in *Eruca sativa*. *Phytochemistry* **65**: 1073–1084
- Fiehn O, Kopka J, Dörmann P, Altmann T, Trethewey RN, Willmitzer L (2000) Metabolite profiling for plant functional genomics. *Nat Biotechnol* **18**: 1157–1161
- Field B, Furniss C, Wilkinson A, Mithen R (2006) Expression of a Brassica isopropylmalate synthase gene in *Arabidopsis* perturbs both glucosinolate and amino acid metabolism. *Plant Mol Biol* **60**: 717–720
- Field B, Guillermo C, Traka M, Botterman J, Vancanneyt G, Mithen R (2004) Glucosinolate and amino acid biosynthesis in Arabidopsis. *Plant Physiol* **135**: 1–12
- Glusker JP, Katz AK, Bock CW (1999) Metal ions in biological systems. *The Rigaku Journal* **16**: 8–17
- Grant M, Smith S (2000) Meeting report; communal weeding. *Genome Biol* **1**: reports 4024.1–4024.3
- Graser G, Schneider B, Oldham NJ, Gershenzon J (2000) The methionine chain elongation pathway in the biosynthesis of glucosinolates in *Eruca sativa* (Brassicaceae). *Arch Biochem Biophys* **378**: 411–419
- Gross SR (1970)  $\alpha$ -Isopropylmalate synthase (*Neurospora*). *Methods Enzymol* **17A**: 777–790
- Hagelstein P, Schultz G (1993) Leucine synthesis in spinach chloroplasts: partial characterization of 2-isopropylmalate synthase. *Biol Chem Hoppe Seyler* **374**: 1105–1108
- Halkier BA, Gershenzon J (2006) Biology and biochemistry of glucosinolates. *Annu Rev Plant Biol* **57**: 303–333
- Hanahan D (1983) Studies on transformation of *Escherichia coli* with plasmids. *J Mol Biol* **166**: 557–580
- Hochuli M, Patzelt H, Oesterhelt D, Wuthrich K, Szyperski T (1999) Amino acid biosynthesis in the halophilic archaeon *Haloarcula hispanica*. *J Bacteriol* **181**: 3226–3237
- Jackson SD, Sonnewald U, Willmitzer L (1993) Cloning and expression analysis of  $\beta$  isopropylmalate dehydrogenase from potato. *Mol Gen Genet* **236**: 309–314
- Junk DJ, Mourad GS (2002) Isolation and expression analyses of the isopropylmalate synthase gene family of *Arabidopsis thaliana*. *J Exp Bot* **53**: 2453–2454
- Kisumi M, Komatsubara S, Chibata I (1977) Pathway for isoleucine formation from pyruvate by leucine biosynthetic enzymes in leucine-accumulating isoleucine revertants of *Serratia marcescens*. *J Biochem (Tokyo)* **8**: 95–103
- Kohlhaw GB (1988)  $\alpha$ -Isopropylmalate synthase from yeast. *Methods Enzymol* **166**: 414–423
- Kohlhaw GB, Leary TR (1970)  $\alpha$ -Isopropylmalate synthase (*Salmonella typhimurium*). *Methods Enzymol* **17A**: 771–777
- Koon N, Squire CJ, Baker EN (2004) Crystal structure of LeuA from *Mycobacterium tuberculosis*, a key enzyme in leucine biosynthesis. *Proc Natl Acad Sci USA* **101**: 8295–8300
- Kroymann J, Donnerhacke S, Schnabelrauch D, Mitchell-Olds T (2003) Evolutionary dynamics of an *Arabidopsis* resistance quantitative trait locus. *Proc Natl Acad Sci USA* **100**: 14587–14592
- Kroymann J, Textor S, Tokuhsa JG, Falk KL, Bartram S, Gershenzon J, Mitchell-Olds T (2001) A gene controlling variation in Arabidopsis



- glucosinolate composition is part of the methionine chain elongation pathway. *Plant Physiol* **127**: 1077–1088
- Leary TR, Kohlhaw GB** (1972)  $\alpha$ -Isopropylmalate synthase from *Salmonella typhimurium*: analysis of the quaternary structure and its relation to function. *J Biol Chem* **247**: 1089–1095
- Lee Y-T, Duggleby RG** (2001) Identification of the regulatory subunit of *Arabidopsis thaliana* acetohydroxy acid synthase and reconstitution with its catalytic subunit. *Biochemistry* **40**: 6836–6844
- Matsuo M, Yamazaki M** (1968) Biosynthesis of sinigrin. VI: Incorporation from homomethionine ( $2\text{-}^{14}\text{C}$ ,  $^{15}\text{N}$ ) and some labelled compounds into sinigrin. *Chem Pharm Bull (Tokyo)* **16**: 1034–1039
- Mifflin BJ, Cave PR** (1972) The control of leucine, isoleucine, and valine biosynthesis in a range of higher plants. *J Exp Bot* **23**: 511–516
- Moore RC, Purugganan MD** (2005) The evolutionary dynamics of plant duplicate genes. *Curr Opin Plant Biol* **8**: 122–128
- Oaks A** (1965) The synthesis of leucine in maize embryos. *Biochim Biophys Acta* **111**: 79–89
- Pátek M, Krumbach K, Eggeling L, Sahn H** (1994) Leucine synthesis in *Corynebacterium glutamicum*: enzyme activities structure of leuA, and effect of leuA inactivation on lysine synthesis. *Appl Environ Microbiol* **60**: 133–140
- Rabin R, Salomon II, Bleiweis AS, Carlin J, Ajl SJ** (1968) Metabolism of ethylmalic acids by *Pseudomonas aeruginosa*. *Biochemistry* **7**: 377–388
- Reichelt M, Brown PD, Schneider B, Oldham NJ, Stauber E, Tokuhisa J, Kliebenstein DJ, Mitchell-Olds T, Gershenzon J** (2002) Benzoic acid glucosinolate esters and other glucosinolates from *Arabidopsis thaliana*. *Phytochemistry* **59**: 663–671
- Roeder PR, Kohlhaw GB** (1980) The  $\alpha$ -isopropylmalate synthase from yeast, a zinc metalloenzyme. *Biochim Biophys Acta* **613**: 482–487
- Rogers SO, Bendich AJ** (1985) Extraction of DNA from milligram amounts of fresh, herbarium and mummified plant tissues. *Plant Mol Biol* **5**: 69–76
- Roessner-Tunali U, Hegemann B, Lytovchenko A, Carrari F, Bruedigam C, Granot D, Fernie AR** (2003) Metabolic profiling of transgenic tomato plants overexpressing hexokinase reveals that the influence of hexose phosphorylation diminishes during fruit development. *Plant Physiol* **133**: 84–99
- Roth M** (1971) Fluorescence reaction for amino acids. *Anal Chem* **43**: 880–882
- Sarwar G, Botting HG** (1993) Evaluation of liquid chromatographic analysis of nutritionally important amino acids in food and physiological samples. *J Chromatogr* **615**: 1–22
- Serif GS, Schmotzer LA** (1968) Biosynthesis of the aglycones of plant thioglucosides—I: precursor studies of the aglycone of progoitrin. *Phytochemistry* **7**: 1151–1157
- Singh BK** (1999) Biosynthesis of valine, leucine and isoleucine. In BK Singh, ed, *Plant Amino Acids*. Dekker, New York, pp 227–248
- Singh BK, Shaner DL** (1995) Biosynthesis of branched chain amino acids: from test tube to field. *Plant Cell* **7**: 935–944
- Somers JM, Amzallag A, Middleton RB** (1973) Genetic fine structure of the leucine operon of *Escherichia coli* K-12. *J Bacteriol* **113**: 1268–1272
- Stieglitz BI, Calvo JM** (1974) Distribution of the isopropylmalate pathway to leucine among diverse bacteria. *J Bacteriol* **118**: 935–941
- Strassman M, Ceci N** (1967) A study of acetyl-CoA condensation with  $\alpha$ -keto acids. *Arch Biochem Biophys* **119**: 420–428
- Textor S, Bartram S, Kroymann J, Falk KL, Hick A, Pickett JA, Gershenzon J** (2004) Biosynthesis of methionine derived glucosinolates in *Arabidopsis thaliana*: recombinant expression and characterization of methylthioalkylmalate synthase, the condensation enzyme of the chain elongation-cycle. *Planta* **218**: 1026–1035
- Ulm EH, Bohme R, Kohlhaw G** (1972)  $\alpha$ -Isopropylmalate synthase from yeast: purification, kinetic studies, and effect of ligands on stability. *J Bacteriol* **110**: 60–89
- Webster RE, Gross SR** (1965) The  $\alpha$ -isopropylmalate synthase of *Neurospora*. I: The kinetic and end product control of  $\alpha$ -isopropylmalate synthetase function. *Biochemistry* **4**: 2309–2318
- Wiegel J** (1978)  $\text{Mn}^{++}$ -specific reactivation of EDTA inactivated  $\alpha$ -isopropylmalate synthetase from *Alcaligenes eutrophus* H16. *Biochem Biophys Res Commun* **82**: 907–912
- Wiegel J** (1981)  $\alpha$ -Isopropylmalate synthetase as a marker for the leucine biosynthetic pathway in several Clostridia and in *Bacterioides fragilis*. *Arch Microbiol* **130**: 385–390
- Wiegel J, Schlegel HG** (1977)  $\alpha$ -Isopropylmalate synthase from *Alcaligenes eutrophus* H16: I. purification and general properties. *Arch Microbiol* **112**: 239–246
- Wittenbach VA, Teaney PW, Hanna WS, Rayner DR, Schloss JV** (1994) Herbicidal activity of an isopropylmalate dehydrogenase inhibitor. *Plant Physiol* **106**: 321–328
- Wittstock U, Halkier BA** (2002) Glucosinolate research in the *Arabidopsis* era. *Trends Plant Sci* **7**: 263–270
- Wu J, Filutowicz M** (1999) Hexahistidine ( $\text{His}_6$ )-tag dependent protein dimerization: a cautionary tale. *Acta Biochim Pol* **46**: 591–599
- Xu H, Zhang Y, Guo X, Ren S, Staempfli AA, Chiao J, Jiang W, Zhao G** (2004) Isoleucine biosynthesis in *Leptospira interrogans* Serotype lai Strain 56601 proceeds via a threonine independent pathway. *J Bacteriol* **186**: 5400–5409
- Zimmermann P, Hirsh-Hoffmann M, Hennig L, Grissem W** (2004) Genevestigator: Arabidopsis microarray database and analysis toolbox. *Plant Physiol* **136**: 2621–2632